# Modeling larval connectivity of the Atlantic surfclams within the Middle Atlantic Bight: Model development, larval dispersal and metapopulation connectivity

Xinzhong Zhang, Dale Haidvogel, Daphne Munroe, Eric N. Powell, John Klinck, Roger Mann, and Frederic S. Castruccio

SEDAR50-RD16

2 May 2016

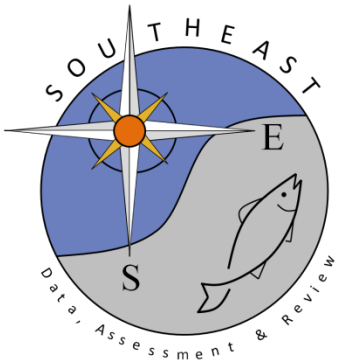

Estuarine, Coastal and Shelf Science 153 (2015) 38–53

Contents lists available at ScienceDirect

Estuarine, Coastal and Shelf Science

journal homepage: www.elsevier.com/locate/ecss

# Modeling larval connectivity of the Atlantic surfclams within the Middle Atlantic Bight: Model development, larval dispersal and metapopulation connectivity

Xinzhong Zhang [a, *], Dale Haidvogel [a], Daphne Munroe [b], Eric N. Powell [c], John Klinck [d], Roger Mann [e], Frederic S. Castruccio [a, 1]

[a] Institute of Marine and Coastal Science, Rutgers University, New Brunswick, NJ 08901, USA
[b] Haskin Shellfish Research Laboratory, Rutgers University, Port Norris, NJ 08349, USA
[c] Gulf Coast Research Laboratory, University of Southern Mississippi, Ocean Springs, MS 39564, USA
[d] Center for Coastal Physical Oceanography, Old Dominion University, Norfolk, VA 23529, USA
[e] Virginia Institute of Marine Science, The College of William and Mary, Gloucester Point, VA 23062, USA

ARTICLE INFO

*Article history:*
Received 19 February 2014
Accepted 30 November 2014
Available online 10 December 2014

*Keywords:*
surfclam (*Spisula solidissima*)
individual-based model
larval transport
connectivity
Middle Atlantic Bight
larval behavior
recruitment

ABSTRACT

To study the primary larval transport pathways and inter-population connectivity patterns of the Atlantic surfclam, *Spisula solidissima*, a coupled modeling system combining a physical circulation model of the Middle Atlantic Bight (MAB), Georges Bank (GBK) and the Gulf of Maine (GoM), and an individual-based surfclam larval model was implemented, validated and applied. Model validation shows that the model can reproduce the observed physical circulation patterns and surface and bottom water temperature, and recreates the observed distributions of surfclam larvae during upwelling and downwelling events. The model results show a typical along-shore connectivity pattern from the northeast to the southwest among the surfclam populations distributed from Georges Bank west and south along the MAB shelf. Continuous surfclam larval input into regions off Delmarva (DMV) and New Jersey (NJ) suggests that insufficient larval supply is unlikely to be the factor causing the failure of the population to recover after the observed decline of the surfclam populations in DMV and NJ from 1997 to 2005. The GBK surfclam population is relatively more isolated than populations to the west and south in the MAB; model results suggest substantial inter-population connectivity from southern New England to the Delmarva region. Simulated surfclam larvae generally drift for over one hundred kilometers along the shelf, but the distance traveled is highly variable in space and over time. Surfclam larval growth and transport are strongly impacted by the physical environment. This suggests the need to further examine how the interaction between environment, behavior, and physiology affects inter-population connectivity. Larval vertical swimming and sinking behaviors have a significant net effect of increasing larval drifting distances when compared with a purely passive model, confirming the need to include larval behavior.


## 1. Introduction[2]

The Atlantic surfclam (hereafter, surfclam), *Spisula solidissima*, is a bivalve mollusk which lives on the continental shelf from shallow subtidal regions to depths of about 60 m, inhabiting the waters from the southern Gulf of St. Lawrence to Cape Hatteras, North Carolina (Ropes, 1980; Cargnelli et al., 1999). The general distribution pattern of surfclams from the Northeast Fisheries Science Center (NEFSC) survey (Fig. 1) indicates that the highest surfclam abundances occur along the New Jersey shelf (NJ), off the Delmarva Peninsula (DMV) and on Georges Bank (GBK). The surfclam is one of the most commercially important species along the Northeast U.S.

* Corresponding author.
*E-mail address:* xinzhong@marine.rutgers.edu (X. Zhang).
[1] Current address: The National Center for Atmospheric Research, Boulder, CO 80301, USA.
[2] Abbreviations used in this article: MABGOM: Middle-Atlantic Bight and Gulf of Maine physical circulation model; MAB – Middle-Atlantic Bight; GBK – Georges Bank; GoM – Gulf of Maine; SVA – South Virginia; DMV – Delmarva; NJ – New Jersey; LI – Long Island; SNE – South New England; NEFSC – Northeast Fisheries Science Center of U.S; ROMS – Regional Ocean Modeling System; IBM – Individual-Based Model; Scl-IBM – Surfclam larval Individual-Based Model.

http://dx.doi.org/10.1016/j.ecss.2014.11.033
0272-7714/

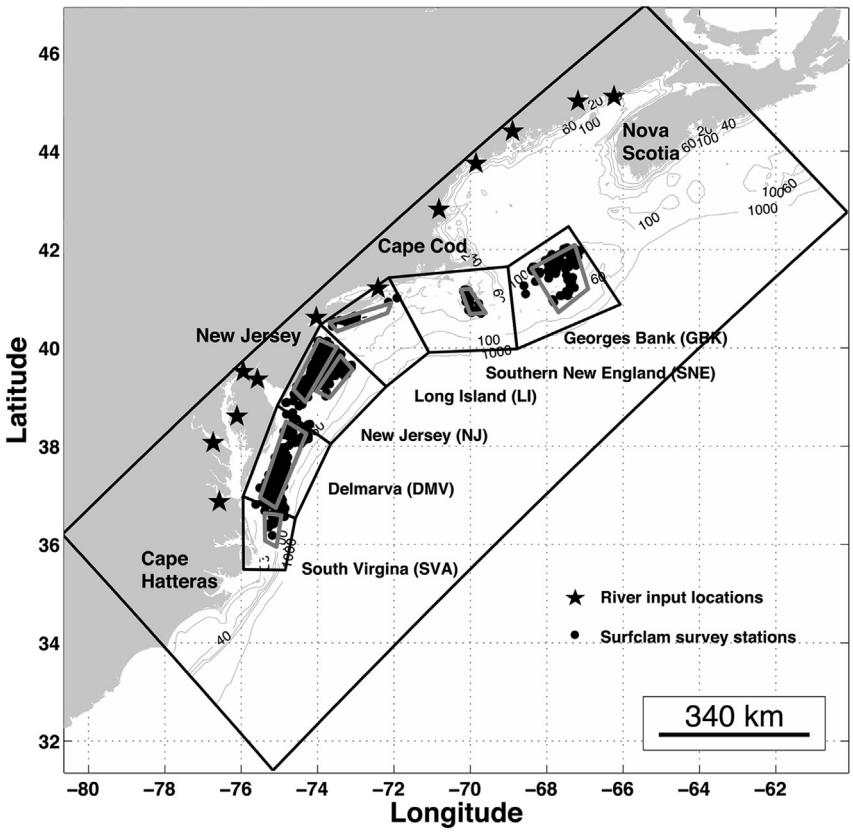


**Fig. 1.** Model domain and distribution of surfclam populations within the Middle Atlantic Bight and Georges Bank. The model domain (shown as the large black rectangular box) is defined by 160 × 120 grid cells and includes 12 rivers. Black stars indicate river input locations. The grid resolution is approximately from 6 to 12 km (the resolution varies about 15% from south to north). Distribution of surfclams in the domain was based on the NEFSC survey data from 1982 to 2008 (NEFSC, 2010) and is shown by black dots representing those survey stations with surfclam density higher than 80 number of clams per survey dredge tow. Black neighboring boxes along the coast represent conventionally used geographic regions for surfclam stock assessments (NEFSC, 2010); these are, from south to north: South Virginia/North Carolina (SVA), Delmarva (DMV), New Jersey (NJ), Long Island (LI), Southern New England (SNE) and Georges Bank (GBK). Gray boxes inside those black regions boxes denote regions of high surfclam density and are used as the larval release regions in the model. Isobaths of 20-, 40-, 60-, 100-, 1000 m are shown as gray solid lines.

coast. Total commercial landings of Atlantic surfclams in 2008 were approximately 28,000 metric tons (mt), with 22,000 mt from federal fisheries and the remainder from state fisheries (NEFSC, 2010).

Recent surfclam stock assessments (NEFSC, 2010) have shown that recruitment of surfclams into the fishable stock has been low in the southern portion of the range off DMV and to a lesser extent off NJ; commercial catch rates and stock biomass also have declined in recent years (1997–2005). In comparison, trends for large surfclam (>120 mm shell length) abundance in the north are either increasing on GBK or variable along the Long Island (LI) and Southern New England (SNE) shelves. These trends in growth and recruitment, particularly off DMV and NJ, remain unexplained; however possibilities include environmental interactions causing poor juvenile survival and slow growth after settlement, high fishing pressure, or discontinuities in larval transport into those areas. Fishing has been suggested to be an unlikely driver of the current period of poor recruitment (NEFSC, 2010); larval transport and connectivity, however, remains an important and as yet understudied aspect of this dynamic.

Similar to many other benthic invertebrates, surfclam life history includes a dispersive larval stage, followed by sessile juvenile and adult stages. Larval dispersal plays a key role in determining connectivity among geographically distinct populations, and is influenced by physical circulation and water properties (Levin, 2006; Cowen and Sponaugle, 2009). Quantitative observation of larval concentration in the ocean is challenging (Underwood and Keough, 2001) and therefore is rarely performed except under conditions that are ideally suited for tracking and observation of marked larvae (e.g., Arnold et al., 2005). As a consequence, numerical modeling has become the method of choice (Peck and Hufnagl, 2012). Numerical modeling has the ability to couple hydrodynamic and larval behavioral models to simulate larval transport, dispersal and growth (Werner et al., 1993; Lough et al., 2005; Savina et al., 2008; Ayata et al., 2009; Narváez et al., 2012a, b) and can therefore serve as a powerful tool for the study of larval dispersal and inter-population connectivity.

Numerical larval models have been in use for various invertebrate species and systems for many years (Leis et al., 2011), including applications examining larval transport on Georges Bank for sea scallops (Tian et al., 2009), the Gulf of Maine lobster (Incze and Naimie, 2000; Xue et al., 2008; Incze et al., 2010), and eastern oysters in Delaware Bay (Narváez et al., 2012a, b) and in Chesapeake Bay (North et al., 2008). Significant advances have been made in numerical modeling techniques; however, more detailed information concerning larval behavior and its interaction with the surrounding physical environment is necessary to further improve individual-based larval models (IBM) and thereby refine model simulations (Miller, 2007).

In this study, we introduce a coupled modeling system combining a physical circulation model and a biological individual-based model developed for Atlantic surfclam larvae. Specific research objectives focus on the development of the coupled modeling system and the determination of the main larval transport pathways and mean larval connectivity patterns for surfclam stocks in the MAB and GBK. These objectives are integral to

management of the Atlantic surfclam fishery. Recent declines in surfclam abundance off Delmarva are thought to be the result of warming of Mid-Atlantic bottom waters in the late 1990s driving an ongoing range shift to the north and offshore (Weinberg et al., 2002; Kim and Powell, 2004; Weinberg, 2005). The failure of surfclams to repopulate southern and inshore waters remains unexplained, as recently observed bottom water temperatures would appear to be within surfclam physiological limits. Thus, a better understanding of larval dispersal in this species may help explain ongoing changes in population abundance and provide increased predictive capability as to the potential of climate change to effect further impacts in this component of the MAB ecosystem.

## 2. Study regions

The Middle Atlantic Bight refers to the U.S. east coast continental shelf region bounded by Cape Hatteras to the south and by Cape Cod and Nantucket Shoals to the northeast (Fig. 1) (Beardsley and Boicourt, 1981). The MAB is a biologically productive region, with several major rivers (e.g., Connecticut River, Hudson River, Delaware River, etc.) that deliver large volumes of fresh water. Most areas in the MAB are relatively shallow. Seasonal variation in water-column stratification in the MAB is significant, with water and nutrients being vertically well mixed during fall and winter, and highly stratified from late spring to summer. These factors combine to induce spring blooms over a wide region and high rates of primary production each year (Schofield et al., 2008), consequently supporting highly productive MAB fisheries, such as the Atlantic sea scallop (*Placopecten magellanicus*), the Atlantic surfclam (*Spisula solidissima*), and the ocean quahog (*Arctica islandica*) that together constitute some of the largest fisheries in the U.S. (Mid-Atlantic Fishery Management Council. 2005).

The general pattern of the time-mean shelf circulation in the MAB exhibits a consistent along-shelf southwestward flow, with depth-averaged barotropic mean velocities observed to be 3–7 cm/s (Beardsley and Boicourt, 1981). The study of the long-term climatology of the mean circulation over the MAB continental shelf shows that the mean equatorward alongshelf barotropic currents are nearly constant along isobaths and increase in speed with shelf water depth. In contrast, the mean across-shelf circulation is relatively weak, but the general vertical structure pattern is consistent (Lentz, 2008).

Georges Bank refers to the large topographic high that bounds the Gulf of Maine and the U.S. northeast continental shelf break east of the Great South Channel, with depths ranging from less than 30 m near the center of the bank to over 300 m at the bank's edge facing the Gulf of Maine (Fig. 1) (Backus, 1987). Tidal rectification and the GBK topography combine to create a year-round clockwise tidal front circulation around GBK on the order of 5–50 cm/s, aligned approximately with the 60-m isobath. The central GBK waters inside the 60-m isobath stay well mixed due to vigorous tidally induced vertical mixing, while surrounding waters get intensively stratified during spring and summer (Csanady and Magnell, 1987). GBK is one of the most physically energetic and biologically productive regions in the world, with annual phytoplankton primary production exceeding 450 g C $m^{-2}$ $yr^{-1}$ in the bank's central portion, historically supporting a lucrative fishery for the Atlantic cod, halibut, haddock, yellowtail flounder, and benthic fisheries like the sea scallop and surfclam (O'Reilly et al., 1987).

## 3. Model development

### 3.1. Physical circulation model

A coastal ocean model (hereafter called MABGOM) incorporating the Middle Atlantic Bight, Georges Bank, and the Gulf of Maine was setup using the Regional Ocean Modeling System (ROMS), a free-surface, terrain-following, primitive equation ocean model widely applied by the scientific community for various applications in both deep ocean and coastal settings (e.g., Haidvogel et al., 2000; Budgell, 2005; Warner et al., 2005; Powell et al., 2006). Resolution of the surface and bottom boundary layers is extremely important for coastal ocean modeling. Vertical stretching in the terrain-following coordinate system used in ROMS enables it to adopt high vertical resolution at the surface and bottom, thereby improving the representation of the surface and bottom boundary layers. Details of the ROMS computational kernel can be found in Shchepetkin and McWilliams (1998, 2003, 2005). Our MABGOM model domain is bounded by Cape Hatteras, North Carolina in the southwest and Nova Scotia, Canada in the northeast, covering the whole U.S northeast continental shelf and also part of the Nova Scotia shelf (Fig. 1).

The atmospheric forcing applied in the model uses National Centers for Environmental Prediction (NCEP) hindcast data. However, when compared with observations measured from the Delaware Environmental Observing System (DEOS) and the Martha's Vineyard Coastal Observatory (MVCO), the NCEP incoming short-wave radiation was found to be consistently ~20% too high in the model domain from the year 2006–2009. Therefore, we applied a 20% reduction to the NCEP incoming short-wave radiation and used this corrected data to force the ROMS model, similar to the correction also done in Wang et al. (2012). The ADvanced CIRCulation model for ocean, coastal and estuarine waters (ADCIRC, Reyns et al., 2006, 2007) is used to provide the tidal forcing at the boundaries of the ROMS domain, whilst observed riverine discharge and water temperature data from U.S. Geological Survey (USGS) are used to prescribe the river runoff.

Following Chen and He (2010), we nested MABGOM within another global ocean circulation model, the HYbrid Coordinate Ocean Model/Navy Coupled Ocean Data Assimilation model, (HYCOM/NCODA) (Bleck et al., 2002), that provides ROMS MABGOM with boundary and initial conditions for temperature, salinity, and barotropic and baroclinic velocities. However, when comparing the HYCOM 4-year (2006–2009) mean temperature and salinity (T&S) with observed MABGOM climatological T&S data (Fleming and Wilkin, 2010), a net bias in both T&S were identified in the HYCOM model data. In particular, HYCOM is approximately 2–3 °C warmer over the entire MAB and GoM, and salinities in HYCOM on the MAB shelf and the Nova Scotia outer shelf are higher by 1 to over 10 (non-dimensional salinity units), especially in Chesapeake Bay, Delaware Bay, and other regions where fresh water inflow is high. The net bias in T&S also causes a bias in the density field, which in turn affects the mean alongshore and across-shelf pressure gradients and currents. We therefore apply corrections to the biased HYCOM model data. Based on observed T&S climatologies (Fleming and Wilkin, 2010), we calculate mean geostrophic transport and barotropic and baroclinic velocities along the model boundary, and use these to correct the HYCOM temporal mean bias, whilst still maintaining the original temporal and spatial variations due to seasonal cycles and various coastal physical processes. These corrected HYCOM boundary and initial conditions are applied to force and initialize the ROMS model.

### 3.2. Surfclam larval individual-based model (Scl-IBM)

The larval model is constructed of two parts, a larval growth sub-model and a larval behavior sub-model, following Dekshenieks et al. (1993, 1996). Implementation of this model structure within ROMS has been used previously to study oyster larval connectivity in Delaware Bay (Narváez et al., 2012a, b; also see North et al., 2008

for a similar model and Leis et al., 2011 for a more general review). Basic clam variables are length (*Len*) in mm, age (*Age*) in days, number (*N*), and depth (*Z*) in meters. Environmental conditions are water temperature (*T*) in °C and larval food (*F*) in mg of dry weight per liter (mg DW/L). The independent variable is time (*t*) in days. The model is an individual-based model that calculates daily the size (*Len*) and depth (*Z*) for a surfclam larva (Peck and Hufnagl, 2012). Those variables used in the model are summarized in Table 1.

### 3.2.1. Growth sub-model

Larval growth data were obtained from laboratory studies (Hurley and Walker, 1996; Hurley et al., 1997; Walker et al., 1998) on *Spisula solidissima* and the surfclam southern subspecies, *S. solidissima similis*, which is considered to be a separate but closely related species (Hare and Weinberg, 2005; Hare et al., 2010). Existing larval data for *S. solidissima* alone were insufficient for model parameterization; therefore laboratory data from both subspecies were used in model parameterization. Recent range extension of *S. s. similis* into Long Island Sound (Hare et al., 2010) suggests that the two subspecies have considerable latitudinal overlap.

In the model, clam length depends on growth rate (*Gr*), which is contingent on three factors: base growth rate ($Gr_{Base}$), which is a function of food (*F*) and *Age*, a correction factor (*CorT*) which depends on water temperature (*T*); and food quality ($F_{Qual}$):

$$Gr(F, Age, T, F_{Qual}) = Gr_{Base}(F, Age) \times CorT(T) \times F_{Qual} \qquad (4.1.1)$$

Larval growth experiments show that growth rate is relatively consistent at optimal standard hatchery feeding rates (Tahitian strain *Isochrysis galbana*, hereafter TIso ≥ 50,000 cells/ml). Data from Renaud et al. (2002) were used to convert cell numbers from experiments to "mg" food (model units). Using these values to solve the above differential equation provides a linear relationship between length and age (Eq. 4.1.2), so that growth rate is constant ($Gr = Gr_0$) if food (*F*) is above a minimal concentration (*Fs*).

$$Len = Gr_0 \times Age + L_0 \qquad (4.1.2)$$

Values of constants ($Gr_0$, $Gr_1$ … $L_0$ etc) are shown in Table 2. Under conditions of starvation, surfclam larvae show limited growth that declines with age (Eq. 4.1.3):

$$Len = Gr_1 \times Age^{Gr_2} \qquad (4.1.3)$$

yielding a growth rate of:

$$Gr_{Base} = \frac{dLen}{dt} = Gr_1 \times Gr_2 \times Age^{(Gr_2 - 1)} \qquad (4.1.4)$$

**Table 1**
List of surfclam larval individual-based model variables.

| Symbol | Name | Units | Notes |
|---|---|---|---|
| *t* | Time | day | |
| *Z* | Larval depth | meters | |
| *T* | Water temperature | °C | |
| *F* | Food concentration | mg DW/L | |
| *Age* | Larval age | day | |
| *Len* | Larval length | mm | See Eqs. 4.1.2, 4.1.3 |
| *Gr* | Larval growth rate | mm/d | See Eqs. 4.1.4, 4.1.5 |
| $Gr_{Base}$ | Base growth rate | mm/d | See Eq. 4.1.1 |
| *CorT* | Temperature effect on growth | | See Eq. 4.1.6 |
| *Sk* | Sink rate | mm/s | See Eq. 4.2.2 |
| *Uss* | Upward swim speed | mm/s | See Eq. 4.2.3 |
| *Usf* | Time fraction swimming upward | | See Eq. 4.2.5 |
| *Dss* | Downward swim speed | mm/s | See Eq. 4.2.4 |

**Table 2**
List of surfclam larval individual-based model constants.

| Symbol | Values | Symbol | Values |
|---|---|---|---|
| $F_{Qual}$ | 1.2 | *Fs* | 1.0 |
| $L_0$ | 58 | *Stf* | 0.920 |
| $Gr_0$ | 8.165 | $S_0$ | $2.220 \times 10^{-4}$ |
| $Gr_1$ | 71.810 | $S_1$ | 1.744 |
| $Gr_2$ | 0.0907 | $U_0$ | −0.381 |
| $Gf_1$ | 0 | $U_1$ | $9.262 \times 10^{-3}$ |
| $Gf_2$ | 0.144 | $U_2$ | $-2.692 \times 10^{-5}$ |
| $Gf_3$ | 1 | $D_0$ | −0.561 |
| $Gf_4$ | 1 | $D_1$ | $1.749 \times 10^{-2}$ |
| $Gf_5$ | 0.144 | $D_2$ | $-6.538 \times 10^{-5}$ |
| $Gf_6$ | 0 | $St_0$ | 21 |
| | | $St_1$ | 0.900 |

If the food concentration is below *Fs*, but above zero, then the growth rate depends on both *Age* and *F* (Eq. 4.1.5, Fig. 2a):

$$Gr_{Base} = Gr_0 \times \frac{F}{Fs} + \left(Gr_1 \times Gr_2 \times Age^{(Gr_2 - 1)}\right) \times \frac{Fs - F}{Fs} \qquad (4.1.5)$$

Temperature also affects growth rate. Larval growth data were available for three temperatures (15, 20 and 25 °C; Hurley and Walker, 1997). High mortality of surfclam larvae at 0 °C and above 30 °C were also reported (Wright et al., 1983; Roosenburg et al., 1984). Goldberg (1989) also noted optimal (maximal) larval growth of surfclams at 20–21 °C. Little information was known for larval growth rates at intermediate temperatures between those anchor points (0, 15, 20, 25, 30 °C). Here in this study we assume linear interpolation to calculate larval growth rates at those intermediate temperatures, and linear extrapolation to presumed zero larval growth at 0 °C and above 30 °C, respectively. Thus, *CorT* is a piecewise fit to temperature effects on growth rate (Eq. 4.1.6, Fig. 2b).

$$\begin{aligned} CorT &= Gf_1 if T \le 10, \\ &= Gf_2 - (Gf_2 - Gf_1) \times \frac{15 - T}{15 - 10} if 10 < T \le 15 \\ &= Gf_3 - (Gf_3 - Gf_2) \times \frac{20 - T}{20 - 15} if 15 < T \le 20 \\ &= Gf_4 - (Gf_4 - Gf_3) \times \frac{25 - T}{25 - 20} if 20 < T \le 25 \\ &= Gf_5 - (Gf_5 - Gf_4) \times \frac{28 - T}{28 - 25} if 20 < T \le 28 \\ &= Gf_6 - (Gf_6 - Gf_5) \times \frac{30 - T}{30 - 28} if 28 < T \le 30 \\ &= Gf_6 if T > 30 \end{aligned} \qquad (4.1.6)$$

Surfclam larvae are thermally sensitive; survival is high at 25 °C, but declines rapidly at 30 °C (Wright et al., 1983; Roosenburg et al., 1984). Temperatures encountered by larvae in the model domain range approximately from 5 to 30 °C; therefore, temperature as a mortality agent was not included in the model.

Lastly, we impose a food quality correction of 1.2, i.e. $F_{Qual} = 1.2$, to increase growth rates enough for settlement to occur in about 25 days at temperatures near 20 °C and a food supply of 1 mg DW/liter, which is more realistic for growth under optimal food conditions (unpublished data) than is a 30-day period that occurs without the correction ($F_{Qual} = 1.0$). This assumes that diets used in reported hatchery experiments on which these rates are based (Tiso) are good, but not optimal diets. Salinity affects larval growth (Hurley and Walker, 1997), but not at salinities encountered on the continental shelf; hence, salinity effects on growth were not included in the model. Growth is debited by the percent time sinking because sinking larvae do not feed.

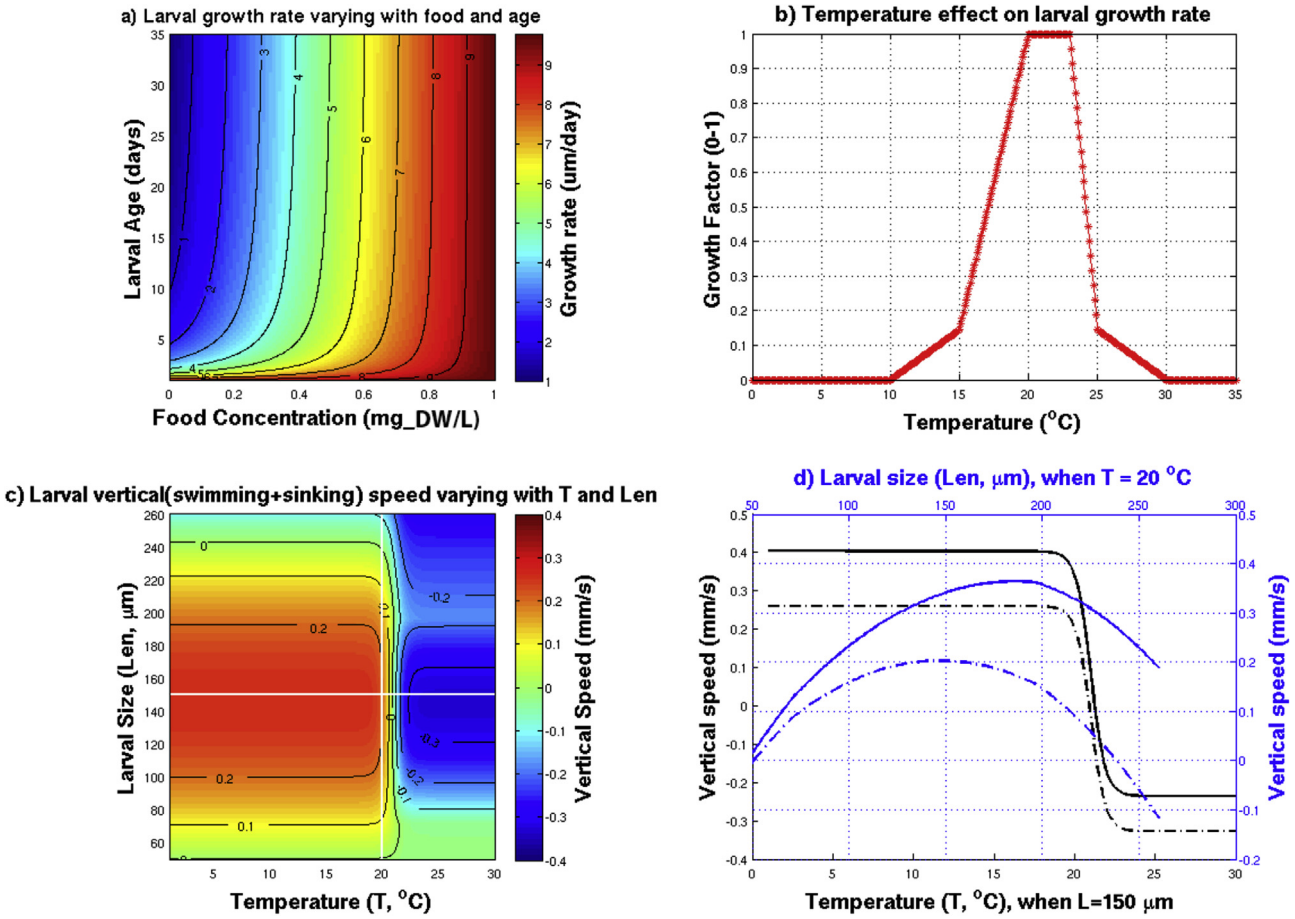


**Fig. 2.** Panel a–b: Variation in modeled larval growth. Panel (a) shows the variability in modeled larval growth rate with food concentration and larval age. The temperature-dependent growth correction factor (*CorT*) is shown in Panel (b); Panel c–d: Variation in modeled larval vertical motion, with positive speed upward. Panel (c) shows the variability in larval vertical motion (swimming + sinking behavior) with temperature and larval size. Panel (d) shows the variability in vertical speed with both swimming + sinking (dashed lines) or swimming only (solid lines) under conditions of varying temperature for larvae of length = 150 μm (lower *x*-axis, black lines), or under varying larval size at temperature = 20 °C (upper *x*-axis, blue lines).

### 3.2.2. Behavioral sub-model

The horizontal swimming speed of larvae is low in comparison with water current speeds, whereas vertical swimming speed is often similar to vertical water movement, and can influence overall larval transport and dispersal (Werner et al., 1993; North et al., 2008), together with the 3D surrounding currents and vertical mixing by diffusion as a random walk motion scaled by the intensity of parameterized turbulence. Larval behavior data were obtained from Mann et al. (1991) who provide upward and downward swimming speeds and sinking speeds as a function of larval length. In addition, Ma et al. (2006a) and Shanks and Brink (2005) provide information on the vertical distribution of larvae on the continental shelf. Observations show that small larvae tend to orient to water near 20 °C and avoid temperatures greater than 22–23 °C or less than 12 °C, and as larvae get larger (nearer to metamorphosis and settlement), they tend to be found deeper in the water column. The temperature dependency was imposed on larval swimming behavior by modifying swimming time up and down as a direct function of temperature, rather than by controlling the swimming and sinking speeds themselves, although either option would have provided the same results.

The vertical speed and direction of movement of the larvae depend on the sinking rate (*Sk*, positive downward), the swimming speed which is a function of length, and the fraction of time spent swimming upward (*Usf*) or downward (*1-Usf*), which is a function of temperature. Larvae do not swim constantly; the fraction of time swimming (*Stf*) was set at 92.5% by tuning simulated larval vertical distributions to field observations. Again, definitions of variables and values of constants used in the model are summarized in Tables 1 and 2 respectively. Combining all of these elements, the net vertical speed is (*Z* is more negative for deeper position):

$$\frac{dZ}{dt} = -Sk(Len) \times (1 - Stf) + Stf \times [Uss(Len) \times Usf(T) - Dss(Len) \times (1 - Usf(T))] \quad (4.2.1)$$

Sinking rate is a function of weight, which is a power function of length, so the sinking rate is:

$$Sk(Len) = S_0 \times Len^{S_1} \quad (4.2.2)$$

The upward swimming speed (*Uss*, positive upward) and downward swimming speed (*Dss*, positive downward) are quadratic functions of length (Mann et al., 1991):

$$Uss(Len) = \max\left(U_0 + U_1 \times Len + U_2 \times Len^2, 0\right) \quad (4.2.3)$$

and

$$Dss(Len) = \max\left(D_0 + D_1 \times Len + D_2 \times Len^2, 0\right) \quad (4.2.4)$$

We assume that larvae respond to ambient temperature (Mann et al., 1991), not the vertical gradient in temperature. Thus, the fraction of time spent swimming upwards depends on the ambient temperature (Fig. 2c,d):

$$Usf(T) = 0.5\left[1 - \tanh\left(\frac{T - St_0}{St_1}\right)\right] \quad (4.2.5)$$

Initial larval size is set equal to egg diameter (58 μm) (Walker and O'Beirn, 1996; Cagnelli et al., 1999). Larvae settle and metamorphose at approximately 260 μm shell length (Fay et al., 1983; Mann et al., 1991; Cargnelli et al., 1999). When larvae are relatively small in size, the vertical swimming behavior dominates in the larval vertical movement, while the sinking behavior becomes dominant when larvae grow large enough (Fig. 2c, d). In the model, settlement occurs at first bottom contact upon reaching this settlement size. The four time-dependent equations are solved with a third-order Adams-Bashforth scheme. The model was verified against data in Ma et al. (2006b) with reference also to Shanks and Brink (2005), and the observed size at settlement. The only tuning required was the percent time swimming, the food quality factor, and the relationship of temperature to swimming speed, where a hyperbolic-tangent relationship was imposed to permit larvae to achieve the observed water column distributions given the observed temperature gradients (Fig. 2c, d).

## 4. Model simulations and analysis

### 4.1. Physical circulation

The ROMS MABGOM model was run for years 2006–2009. For this study, temperature and coastal currents are the most important physical circulation features (see Section 3). Therefore, the mean circulation field and the mean surface and bottom temperature fields from the model output were analyzed and validated by comparison with available observational data. In this study region, the Gulf Stream is an important dynamic feature, as its mean path and variation can cause large variations in the MAB shelf water properties (Churchill et al., 1993). Therefore, the simulated and observed mean Gulf Stream paths have also been compared.

### 4.2. Larval release strategies

The surfclam larval model was coupled with the physical circulation model for the years 2006–2009. A similarly coupled shellfish larval submodel, an oyster larval model, is currently available to the public as a new capability within ROMS, and more details about the coupling method can be found in Narváez et al. (2012a, b).

Surfclam spawning ranges from late spring (late May or June) until fall (Ropes, 1968; Jones, 1981; Fay et al., 1983; Cargnelli et al., 1999). Accordingly, simulated larvae were released throughout the spawning season at 5-day intervals from May 21st until October 16th, generating a total of 30 release times in each year. Larval release locations are defined in the model following the observed surfclam population distribution pattern (Fig. 1). A map of surfclam abundance from 1982 to 2008 NEFSC surfclam stock surveys (NEFSC, 2010) shows the 7 major geographic regions with large surfclam stocks (blue boxes in Fig. 1), namely from south to north: South Virginia/North Carolina (SVA), Delmarva (DMV), New Jersey inshore (NJ_in), New Jersey offshore (NJ_off), Long Island (LI), Southern New England (SNE) and Georges Bank (GBK). The New Jersey region was divided into offshore and inshore components in this study to permit investigation of the offshore shift in range identified by Weinberg et al. (2005). The numbers of larvae released from within each of these regions was calculated by multiplying the average clam density (numbers/tow) in each region by its area. This assumes that the number of larvae released within each region is proportional to the local adult clam density. The derived population numbers for region (SVA, DMV, NJ_in, NJ_off, LI, SNE and GBK) are 400, 2000, 1800, 300, 400, 400 and 1500, respectively. These numbers of surfclam larvae are then approximately evenly released within each box simultaneously at midnight of the selected release dates. The release depth was the bottom-most grid cell. Therefore, a total of 204,000 larvae (6800 per release) were released each year, covering the spawning season and all the major surfclam spawning regions on the Northeast U.S. shelf.

In addition to the physical fields that the circulation model provided for the surfclam larval model, we also set the food concentration ($F$, in mg DW/liter). Reliable field estimates for larval food are unavailable (Munroe et al., 2013); therefore, food concentration was set to be an optimal constant value (1 mg DW/liter), on the assumption that surfclam larvae never lack food in the water. Thus, times to settlement for these simulations are minimal given the temperatures to which the simulated larvae were exposed.

### 4.3. Larval transport, connectivity, and behavioral sensitivity

Metamorphosis for surfclams occurs from 19 to 35 days depending on temperature during larval growth (Fay et al., 1983). Given our assumption that food supply is not limited for simulated larvae, we further assume that the maximum duration of the larval stage for successfully recruiting larvae is 35 days. Additionally, nearly all adult surfclams are found shallower than 60 m (NEFSC, 2010, Fig. 1). Thus, in the model we define successful larvae as those that i) reach settlement size (260 μm) within 35 days of release to complete settlement and ii) do so within potential settlement habitat (shallower than the 60 m isobath) anywhere on the shelf.

The along-shore and across-shelf drift for each larva were calculated by comparing the release position and the point of final settlement, or the place where the larva was at the end of 35 days if it had not yet successfully settled. The mean drifting pattern among all the larvae released at the same time from the same region was calculated and used to determine the average larval connectivity pattern for all 4 years. The connections among the different geographically distributed subpopulations are illustrated with a connectivity matrix. The connectivity matrix is computed between each of the 6 along-shelf regions (black boxes in Fig. 1), showing the percentage of larvae released from one region that arrive and settle into the same region or the other regions.

Larvae are transported by the simulated 3D currents, vertically mixed by diffusion as a random walk motion scaled by the intensity of parameterized turbulent mixing, and also larval behaviors. To test the importance of larval behavior, both vertical swimming and sinking, on transport and connectivity, additional simulations were performed for year 2006: a) with only larval vertical swimming, b) with only larval vertical sinking, and c) with neither (purely passive). In the “swim only” simulation (a), the larval sinking behavior was turned off and larvae were assumed to be swimming continuously in the vertical direction, while in the “sink only” simulation (b), the larval swimming behavior was turned off but larvae were still allowed to grow and to sink at the rate dependent on larval size. In the “purely passive” simulation (c), larvae are only transported as passive neutrally-buoyant particles without swimming and sinking behaviors, but can still grow and reach settlement size.

The resulting mean larval drifting distances in these simulations were calculated in the same way as previously described, and were compared with the results of the initial 2006 simulation with both larval swimming and sinking behaviors in the model.

## 5. Results

### 5.1. Model validation

#### 5.1.1. Physical circulation model

Daily values of temperature, salinity, sea surface height, and barotropic and baroclinic current velocities are obtained from a 4-year ROMS MABGOM simulation. The 4-year average of sea surface temperature (at 1-m depth) and barotropic current fields were calculated from the model output (Fig. 3a). The path of the Gulf Stream (GS) can be detected readily by the mean sea surface temperature (SST) 21 °C isotherm. Comparison of the GS path between the model (green line) and observation (blue line) shows good agreement where the GS flows into and out of the model (Fig. 3a, b). The mean barotropic currents on the MAB shelf and GBK southern flank in the model flow generally southwestward along the coast, with both magnitude and direction consistent with the long-term mean climatological observations (Lentz, 2008, Fig. 3a). On the southern flank of GBK, simulated mean barotropic currents reach close to 0.09 m/s, while along the NJ and DMV shelf break they also approach 0.1 m/s. The inner shelf mean southwestward flow is slower than the shelf break current, at around 0.03–0.04 m/s. The model barotropic zonal and meridional current biases are approximately 0.0003 m/s and 0.0061 m/s respectively (model - climatology), which indicates good consistency ($p$-value $< 1 \times 10^{-10}$). The physical circulation model is thus found to adequately capture the main pattern of the MAB shelf current system. Considering surfclam larval span of around 35 days, these biases in the barotropic currents might contribute to the maximum of 18 km larval alongshore drifting distance error, which is small relative to the scale of management areas in more than 150 km.

Model output for the 4-year mean SST from year 2006–2009 is compared to satellite observations in Fig. 3a,b. This comparison shows reasonable agreement for both the Gulf Stream region and the MAB shelf. The simulated surface and bottom temperatures during late-spring to early-fall in 2006–2009 are compared with Northeastern Fishery Science Center (NEFSC) observations (NEFSC Oceanography Branch CTD Data Reports, 2006–2009) in Fig. 3c,d. Model temperature biases (model-observation) at the surface and bottom are about 0.15 °C (RMS = 1.32 °C) and −0.32 °C (RMS = 2.03 °C), respectively. In general, this comparison shows acceptable consistency between model results and observation, assuring that the model reproduces the main MAB shelf water surface and bottom temperature distributions with accuracy sufficient for the requirements of the Scl-IBM. Sporadic and sparse dots with relatively larger temperature differences (around ± 5 °C) between model results and observations are also detected (Fig. 3c,d), especially close to the shelf break regions where Gulf Stream meanders might cause large temporal and spatial

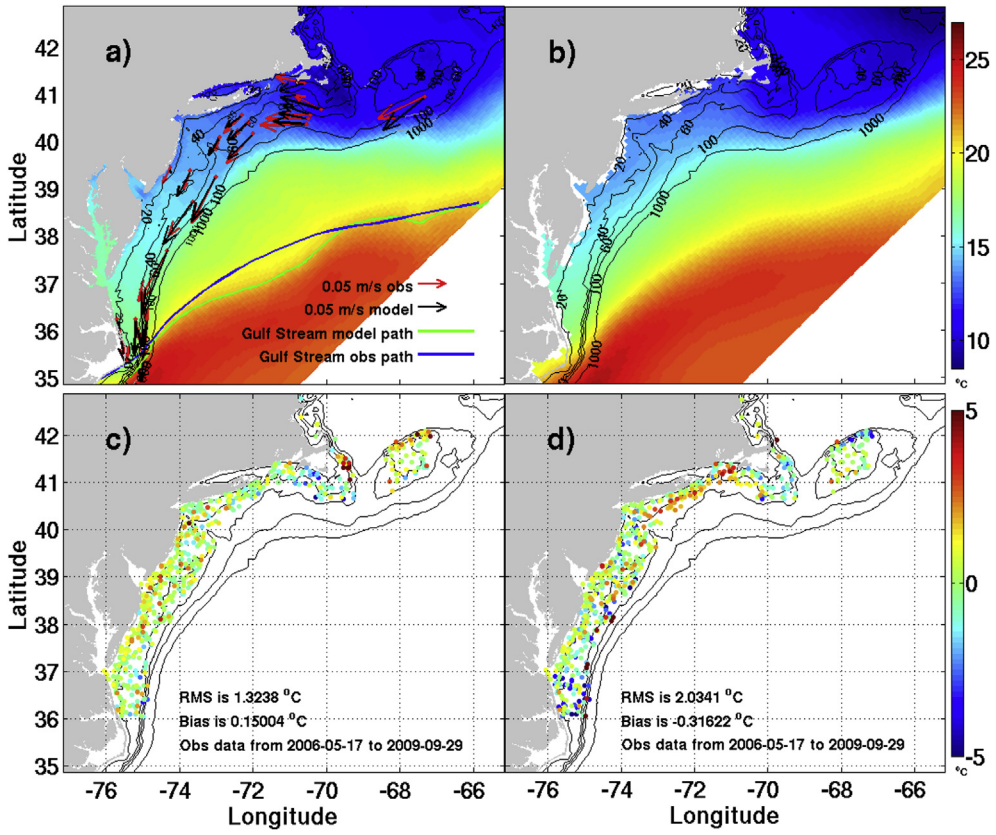


**Fig. 3.** Panel a–b: Comparison of modeled 4-year mean SST at 1-m depth (Panel a) and satellite observed 4-year mean SST (Panel b) (Reynolds et al., 2007) from year 2006–2009, as indicated by the colorbar on right. In Panel a, the green line indicates the 21 °C SST isotherm from the mean simulated SST (used here as a proxy of the modeled Gulf Stream location), and the blue line shows the 21 °C SST isotherm based on mean observed SST over the same period (Reynolds et al., 2007). The comparison between the 4-year mean barotropic currents (black arrows) from model output and the long-term mean climatological barotropic currents (red arrows) (Lentz, 2008) is also shown in Panel a. Panel c–d: Comparisons of surface (Panel c) and bottom (Panel d) temperature between model output and NEFSC observational data during late-spring to early-fall from 2006 to 2009. Colorbar on the right shows the temperature differences (model − observation in °C), at each survey station on the corresponding survey date. In all panels, the 20-, 40-, 60-, 100-, 1000-m isobaths are also shown as black lines.

variations. This might be attributed to the difficulty that numerical models traditionally have in capturing the exact variability of Gulf Stream meanders due to the dynamic complexities and high non-linearities involved (Miller and Lee, 1995).

### 5.1.2. Larval model validation

In the coupled modeling system, larval trajectories allow us to observe larval transport and horizontal and vertical distributions. Observational data of the distribution of surfclam larvae in the ocean are rare, making it difficult to validate the larval model in a fashion similar to that used for the physical model. However, detailed observations of larval distributions along an across-shelf section at the New Jersey LEO-15 observatory (Long-term Ecosystem Observatory, Fig. 4) during upwelling and downwelling periods do provide sufficient detail for qualitative validation (Ma et al., 2006a), and thus were used to compare modeled larval distributions for the same location within the model domain. Observations show that during upwelling, surfclam larvae tend to concentrate near the thermocline, while during downwelling they concentrate close to the intersection of the thermocline and the bottom (Fig. 4 in Ma et al., 2006a). Modeled larval distributions followed the same pattern during upwelling and downwelling (Fig. 4), indicating that the coupled modeling system is faithfully reproducing surfclam larval behavior and water-column vertical distribution.

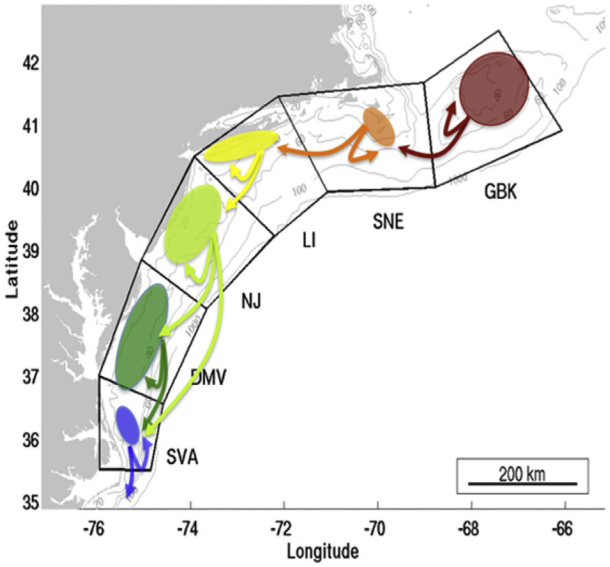


**Fig. 5.** Horizontal (panel a) and vertical (panel c) larval trajectories of an individual larva released along the southern New Jersey shelf on August 1, 2006. In Panel a, the green dot represents the final larval settlement position. Isobaths of 20-, 40-, 60-, 100 m are shown in black solid lines. In Panel c, the colorbar indicates the background water temperature. Panel b shows the size of the larva as it grows over time.

### 5.2. Larval transport and population connectivity

As an example, we follow the horizontal and vertical transport trajectory (Figs. 5a,c) growth history (Fig. 5b) for an individual larva released along the southern New Jersey shelf on Aug. 1st, 2006. This larva spends about 35 days in the water column. At day 35, it reaches settlement size (260 μm) and settles to the bottom. In the horizontal, this larva was transported southwestward along the shore following the coastal current and eventually settled close to the mouth of Chesapeake Bay. In the vertical, this larva quickly swims upward after release and spends most of the larval stage close to the thermocline, near the 20–21 °C isotherm (Fig. 5c), the preferred temperature range for surfclam larval growth. Some abrupt larval vertical movement related to strong turbulence events are obvious when the larva drifts close to the Delaware Bay mouth (Fig. 5c). Close correlation between the variation in larval transport and the surrounding coastal current pattern indicates a strong influence of the physical environment on the larval position and performance.

Focusing on the entire population of larvae shows that average larval transport is to the southwest. The mean larval transport and connectivity pattern in MAB and GBK can be generalized as shown in Fig. 7. In this example taken from the August 1st, 2006 release (Fig. 6a,b), almost all the larvae released in the model domain are transported southwestward along-shore, except for some released from DMV and SVA that are entrained into the Gulf Stream and transported northeastward into the open ocean where they can be expected to die (Fig. 6b). Connectivity is highest between adjacent management regions. In each region, most recruiting larvae either originate from their release region (self-recruits) or from the neighboring region upstream. For example, in the August 1st, 2006 release, most larvae released in LI were finally transported into the NJ region, while most larvae released in NJ were transported into the DMV region, and so on. The mean subpopulation connectivity matrix (Fig. 8) summarizes this finding.

Two different 4-year-mean connectivity matrices were calculated for larval transport after 35 days post-release. The first

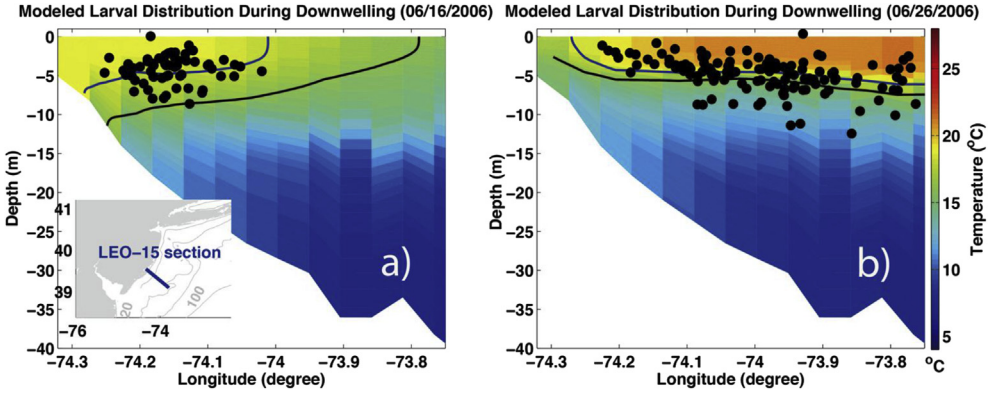


**Fig. 4.** Modeled surfclam larval distribution along the New Jersey LEO-15 across-shelf section during downwelling (June 16th 2006, panel a) and upwelling periods (June 26th 2006, panel b) in 2006, with each dot representing each larva in the water. The 16 °C (lower black line) and 18 °C (upper black line) isotherms are shown to indicate the approximate thermocline positions. The bottom left inset of panel a shows the location of the LEO-15 transect (blue line) off NJ shelf.

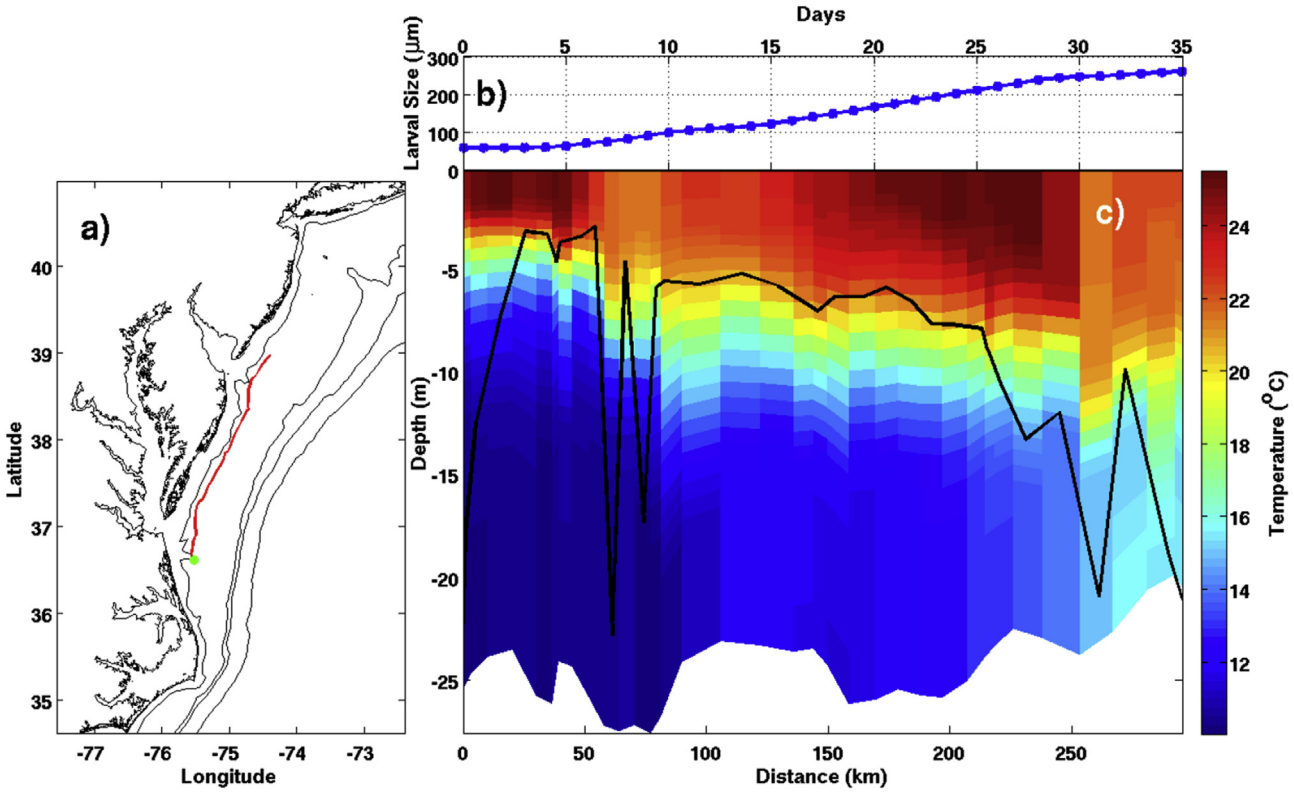


**Fig. 6.** Larval distribution on September 5, 2006, 35 days after larval release on August 1. Panel a shows the distribution of all larvae from the initial release, including those that settled successfully and those that did not. Panel b shows the distribution of only those larvae able to successfully settle within the 35-day limit. Each dot represents one larva and colors indicate initial release locations as follows: GBK-pink, SNE-black, LI-yellow, NJ inshore-green, NJ offshore-light blue, DMV-blue, SVA-red. Lower right inset in panel b shows the initial distribution of the larvae at the time of release.

matrix shows the overall pattern of larval supply, which is defined as the portion of larvae transported from one region to another (Fig. 8a). The second matrix indicates the pattern of larval settlement, defined as the portion of larvae from one region that were both transported and successfully settled in another (Fig. 8b). The connectivity pattern is similar in both matrices, but with different magnitudes. Diagonal trends in both matrices are obvious, indicating good larval retention within each geographic region and significant self-settlement. The off-diagonal values in the lower half are relatively larger than the analogous values in the upper half, confirming that larvae are generally transported from upstream (north and east) regions into downstream (south and west) regions, forming a southwestward connection pattern. Thus, pairs of adjacent geographic regions typically show substantial connectivity, as revealed by the values in cells below the diagonal in the matrix, and often these larvae provide more settlement potential than those derived locally. For instance, on average, 43.4% of all larvae released in NJ are transported into DMV while 45.6% remain on the NJ shelf (Fig. 8a), and 20.2% of all larvae released in NJ reach settlement size in DMV whereas 19.7% reach settlement size on the NJ shelf (Fig. 8b). Compared to the MAB geographic regions, GBK is relatively more isolated, with little

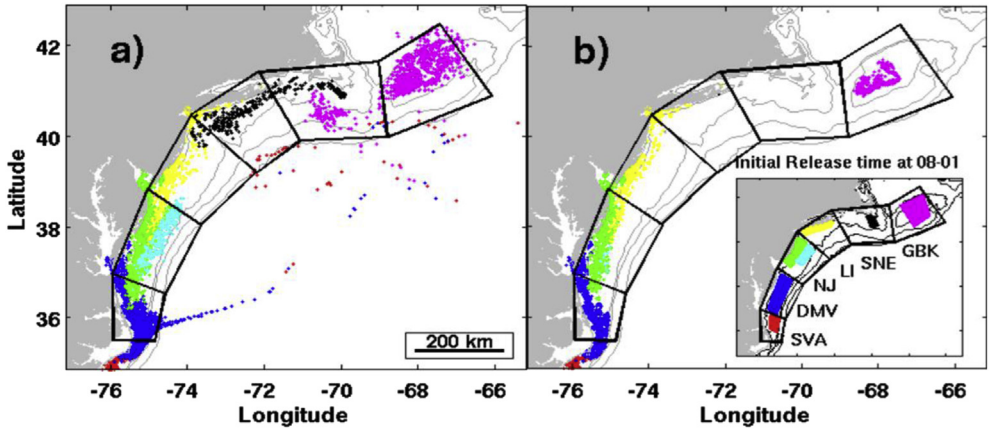


**Fig. 7.** Generalized mean connectivity pattern between the MAB and GBK surfclam subpopulations based on the model output for all releases in 2006–2009.

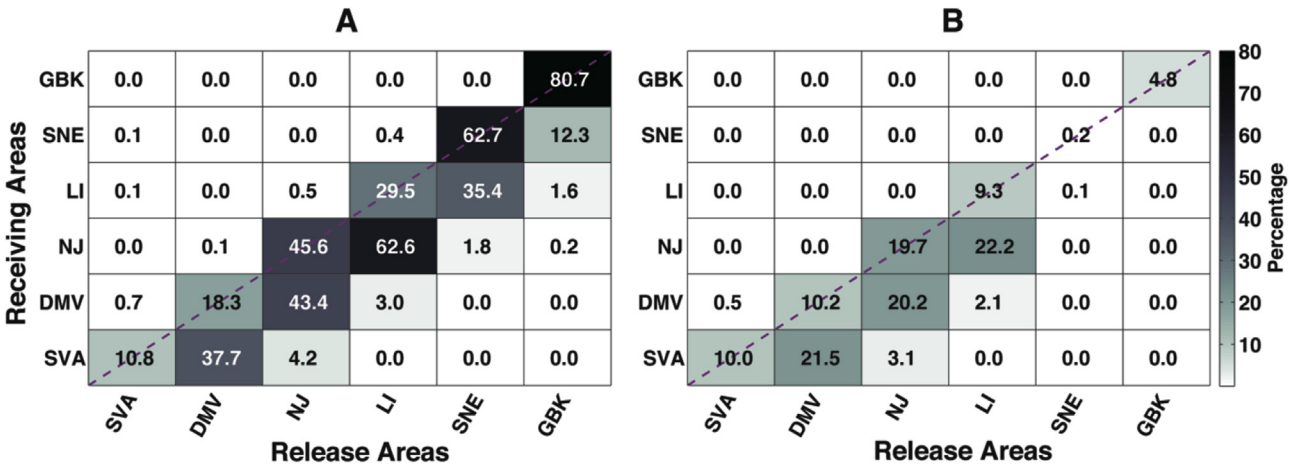


**Fig. 8.** Four-year (2006–2009) mean modeled connectivity matrix among the 6 main surfclam geographic regions: SVA, DMV, NJ, LI, SNE and GBK, showing the percentage of larvae released in one region (*x* axis, see Fig. 1 for their locations) that are transported (larval supply, panel A) or successfully settled (larval settlement, panel B) into the same or another region (*y* axis, see Fig. 1 for their locations). The exact percentage values are indicated by both the colorbar and the text in each cell. Both panels indicate the results without daily mortality applied.

larval transport to other regions and very few immigrants from other regions.

### 5.3. Larval drifting distances and behavior effects

Surfclam larval drifting distances calculation was indicated previously in Section 4.3. On average, surfclam larvae drifted 119 km (±94 km st. dev.) southwestward along-shore, and 5 km (±17 km st. dev.) inshore (perpendicular to the coast). Large variations of both along-shore and across-shelf larval drifting distances exist among larvae released from different regions (Fig. 9a, b). In the along-shore direction, larvae released in DMV experienced the longest southwestward drift, while those released from GBK experienced the shortest along-shore drifting distance, which is intuitively understandable because of the clockwise gyre on the bank that reduces along-shore drift. In the across-shelf direction, larvae released from the SVA, DMV, and NJ regions experienced onshore drifting with median distances over 10 km, while larvae released in LI and SNE experienced predominantly offshore drifting with median distances of 1.5 km and 6 km respectively, and the GBK larvae experienced almost no across-shelf drifting on average. In addition, statistical tests show significant across-region differences in the temporal variances of larval drifting distances in both along-shore and across-shore directions. For the along-shore larval drifting distance, larvae released from NJ, LI, and SNE experienced about 1.5–2 times larger temporal variances than those released from SVA, DMV, and GBK (Fig. 9a). For the across-shore larval drifting distance, larvae released from GBK experienced about 3–5 times larger temporal variances than those released elsewhere (Fig. 9b).

The results of simulations to examine the sensitivity of larval trajectories to larval behavior indicate that both larval swimming and sinking behavior significantly influence larval along-shore drifting (Fig. 9c). On average, larval swimming behavior increases the along-shore southwestward drifting distances by about 56 km ($F = 45923$, $n = 244341$, $p$-value $< 1 \times 10^{-10}$), whereas larval sinking behavior decreases the along-shore drifting distances by about 26 km ($F = 8929$, $n = 246293$, $p$-value $< 1 \times 10^{-10}$). In the standard model configuration with both swimming and sinking behaviors (Fig. 9c, magenta color), the combined effects of both behaviors increase the mean larval drifting distance by about 30 km ($F = 6220$, $n = 121219$, $p$-value $< 1 \times 10^{-10}$) compared to the distance achieved by purely passive transport (Fig. 9c, cyan color). In addition, statistical tests show that both larval swimming and sinking behaviors affect the temporal variances of larval along-shore drifting distances in a significant way, with larval swimming behavior increasing the temporal variance and the sinking behavior decreasing the variance (Fig. 9c).

## 6. Discussion

### 6.1. Larval transport and connectivity

The model results indicate a mean upstream-downstream (northeastward-southwestward) surfclam larval transport and connectivity pattern, which is mainly driven by the mean shelf current flowing southwestward (Fig. 3a). For most surfclam geographic regions, larval supply comes from larvae retained in the region or released from the region immediately upstream. Thus, variability in the number of larvae released from an upstream region can be expected to be a significant factor in determining the number of larvae settling in the adjoining downstream region.

Another factor influencing the contribution of larval supply from the local and upstream regions is temporal variability, both seasonally and inter-annually, in larval transport (Zhang et al., 2015). Here, we have considered the average larval transport patterns over the entire spawning season and over 4 years from 2006 to 2009; however our observations, and those of others (Xue et al., 2008; Tian et al., 2009; Narváez et al., 2012a, b), indicate that physical and environmental changes can cause strong temporal variability in larval supply. A great deal of individual variation also exists among larval release times within a given region and between regions (Figs. 9a, b). For example, larvae released from SVA, DMV, and GBK experienced smaller temporal variances in the along-shore drifting distances than those released from NJ, LI, and SNE (Fig. 9a), potentially related to the fact that larvae released from SVA and DMV generally stay deeper in the water column and experience less along-shore current variations (Zhang et al., 2015), and that the GBK around-bank circulation retains most larvae on the bank. The same factor on GBK is the likely cause of the larger variance in the across-shore larval drifting distances for larvae released on GBK. This variability is the topic of additional research using this coupled modeling system (Zhang et al., 2015), and also suggests the need to further examine in detail how the physical

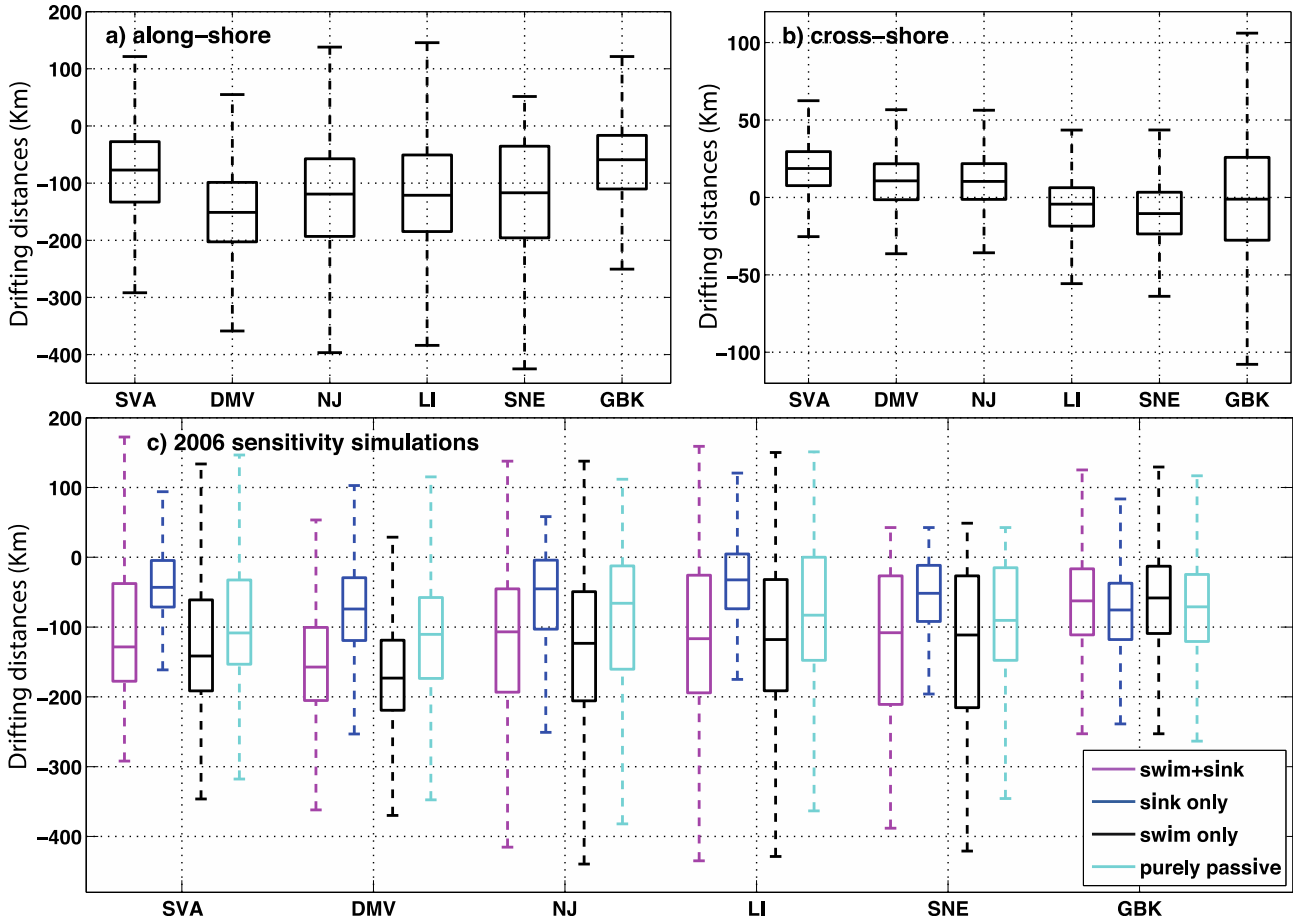


**Fig. 9.** Panel a–b: Box-plots showing median, ±25% quantiles and extreme values of larval drifting distances (units: kms; *y*-axis) in the along-shore (panel a) and across-shelf (panel b) directions for all released larvae from regions of SVA, DMV, NJ, LI, SNE and GBK (*x*-axis) in 2006–2009. Along the *y*-axis, positive values indicate southwestward along-shore drifting, or onshore across-shelf drifting; negative values indicate the opposite direction. Panel c: Box-plots of larval drifting distances (units: kms; *y* axis) in the along-shore direction for all released larvae from regions of SVA, DMV, NJ, LI, SNE and GBK (*x* axis) in 2006, with both swimming and sinking behaviors (magenta: swim + sink, the standard model setup), only sinking behavior (blue: sink only), only vertical swimming behavior (black: swim only), and neither (cyan: purely passive).

environment impacts larval growth, transport and population connectivity.

In this study, this larval settlement connectivity matrix (Fig. 8b) shows a continuous, although variable, surfclam larval input into the SVA, DMV, and NJ regions, either through the retention of larvae spawned in that region or the transport of larvae from regions upstream (particularly the immediately upstream region). This suggests that insufficient larval supply and settlement is an unlikely cause for the failure of the surfclam population to recover after the decline in DMV and NJ observed from 1997 to 2005 because larvae would have likely been supplied from upstream populations that had not coincidentally declined. Factors such as poor juvenile survival and slow growth after larval settlement are more likely explanations (e.g., Quijón et al., 2007).

The connectivity matrix shows few larval settlements among those released from SNE into SNE itself and LI, about 0.3% in total on average in 4 years (Fig. 8b). In the example of the August 1st, 2006 release, few larvae released from SNE finally settled (Fig. 6). This might not reflect reality. O'Connor et al. (2007) suggest that larval survival is lower at colder temperatures for most marine planktonic larvae because slower growth rates at lower temperatures extended the planktonic larval duration. In this surfclam model, the decline in the fraction of larvae reaching settlement size by 35 days at higher latitudes such as SNE and GBK is due less to the failure of larvae to be available in these regions as it is to failure of larvae to reach settlement size in 35 days. This effect results directly from the lower temperatures of surface waters at higher latitudes that slow growth rates of the simulated larvae. Our larval model assumes that larval mortality rates are sufficiently high that few larvae will survive much longer than 35 days. If larval mortality rates are lower than routinely assumed (see for example, Rumrill, 1990; Johnson and Shanks, 2003; Short et al., 2013) permitting considerable larval survival beyond 35 days, settlement rates would be higher than indicated in the connectivity matrices presented in Fig. 8b. A similar argument also applies to those larvae released from NJ offshore, as model results show few larvae settling from those larvae released from NJ offshore and the bottom temperature at NJ offshore is colder than inshore (Castelao et al., 2008).

The model shows little connection between the GBK surfclam subpopulation and others to the west and south (Figs. 6 and 8b). Georges Bank (GBK) is becoming an increasingly important region for the surfclam fishery after it was reopened after a lengthy closure since 1989 due to the occurrence of Paralytic Shellfish Poisoning (PSP) (NEFSC, 2010). However, our modeling results suggest that the GBK surfclam fishery reopening might only have limited influence on the MAB subpopulations as a spawning stock to support regions downstream. In terms of human fishing, the shift of fishery efforts onto the bank could be important in easing the fishing pressure on NJ and DMV and help populations there to recover.

### 6.2. Larval drifting distances and behavioral effects

On average, simulated surfclam larvae drifted over one hundred kilometers southwestward along the shelf (Table 3). In a meta-analysis of correlation between larval duration and observed drifting distances, Shanks (2009) demonstrated that nearly half of the observed variability in drift distance can be explained by pelagic larval duration. The drift distances for surfclams estimated by this model are comparable to model estimates of drifting distances of sea scallop larvae on Georges Bank (Tian et al., 2009) and lobster larvae in the Gulf of Maine (Incze and Naimie, 2000). These three species inhabit the continental shelf, and all have larval life spans near one month. In contrast, model estimates of larval drifting distances for oysters in east coast estuaries are found to be 80–90% shorter, in the range of only 10–30 km (North et al., 2008; Haase et al., 2012; Narváez et al., 2012b), even though their larval durations are comparable to the continental shelf species (e.g., Dekshenieks et al., 1993). In a comparison of observed dispersal distances for sympatric species from the US Pacific Coast, López-Duarte et al. (2012) similarly found that oyster larva planktonic duration was twice that of mussels, yet the dispersal distances were half as far. Thus, besides pelagic larval duration, other potential factors contributing to the larval drifting distance vary between these taxa, such as differential larval behavior and properties of the physical environment that they inhabit. Species that live in estuaries often develop complex behaviors such as vertical migrations with daily or lunar periodicity, that allow them to be carried preferentially in water masses that keep them near or return them to natal habitats, thereby reducing overall drift distances (Tilburg et al., 2010; Miller and Morgan, 2013). Salinity gradients are also important (Dekshenieks et al., 1996) whereas they exert little influence on the shelf. Additionally, estuarine water is typically more mixed and the current more variable causing larvae to experience less drifting, whereas on the shelf the physical environment is less variable so that drifting larvae are carried greater distances.

In general, model estimates of passive larval drift tend to predict longer than observed distances of travel (Shanks, 2009), supporting the current paradigm that larvae are retained at a greater rate than would be expected based simply on physical transport (Levin, 2006; Cowen and Sponaugle, 2009; López-Duarte et al., 2012). This paradigm derives from comparisons between model predictions using both passive models and those including behavior, and observations of dispersal distances (Shanks, 2009). Results of sensitivity simulations performed in this modeling study show that surfclam larval vertical swimming behavior increases the mean larval drifting distances by permitting larvae to access stronger horizontal surface currents. In contrast, larval sinking behavior permits larvae to sink deeper into the water column and experience slower bottom current and shorter drifting distances. The combined effects of both vertical swimming and sinking increased larval drifting distances by around 25%, contrary to the general trend in which larval behavior decreases drifting distances for many other species (Shanks, 2009; López-Duarte et al., 2012). This difference might be attributable to different mechanisms controlling larval behavior that were not included here. In this study larval behavior is based only on water temperature, while more complex behaviors can be generated by interaction with the background currents, salinity, turbulence, light, gravity and pressure that could create greater larval retention and shorter dispersal distances (Largier, 2003; Shanks, 2009; Miller and Morgan, 2013). However, longer drifting distances may be valuable to a widely distributed open shelf species such as the surfclam. Whether the longer dispersal distances we predict with the addition of larval behavior to the model is truly a reflection of realistic conditions or not, it is noteworthy in that it is an unexpected and contradictory result

**Table 3**
Summary of recently published larval transport model studies for benthic species along the U.S northeast coast.

| Species | Study Region(s) | Physical circulation model | Larval behavior | Model coupling method[a] | Pelagic duration | Larval drifting distances | References |
|---|---|---|---|---|---|---|---|
| Atlantic surfclam (*Spisula solidissima*) | Georges Bank, Middle Atlantic Bight | Regional Ocean Modeling System (Haidvogel et al., 2000) | 1. Growing,<br>2. Vertical swimming and sinking | In-line | ~19–35 days | ~119 km (mean along-shore) | This study |
| Sea scallop (*Placopecten magellanicus*) | Georges Bank, Middle Atlantic Bight | Finite-Volume Coastal Ocean Model (Chen et al., 2001) | 1. Vertical swimming<br>2. Habitat selection by settlement probability | Off-line | ~40–50 days | As long as hundreds of kilometers | Tian et al., 2009 |
| Lobster (*Homarus amerianus*) | Gulf of Maine | Dartmouth Circulation Model (Lynch et al., 1996, 1997) | 1. Growing<br>2. Constant larval depth | Off-line | ~18–38 days | ~19–280 km | Incze and Naimie, 2000 |
| | Gulf of Maine | Princeton Ocean Model (Mellor, 2003) | 1. Growing<br>2. Ontogenetic changes in vertical distribution | Off-line | ~22–44 days | – | Xue et al., 2008 |
| Eastern oyster (*Crassostrea virginica*) | Delaware Bay | Regional Ocean Modeling System (Haidvogel et al., 2000) | 1. Growing,<br>2. Vertical swimming and sinking | In-line | <30 days | Mostly 0–20 km | Narváez et al., 2012b |
| | Chesapeake Bay | Regional Ocean Modeling System (Haidvogel et al., 2000) | 1. Vertical swimming | Off-line | ~14–21 days | ~9.0 km (median distance) | North et al., 2008 |
| | Pamlico Sound, North Carolina | Advanced CIRCulation model (Reyns et al., 2006, 2007) | None, with larvae constrained at constant depth | Off-line | ~14–25 days | ~0.3–35.8 km | Haase et al., 2012 |

[a] Model coupling method: "Inline" indicates that the physical model and biological model are embedded such that both models are running simultaneously, while "Offline" indicates separate computations, usually with the physical model run first, then providing the necessary circulation fields to the biological model.

when compared to most studies. Surfclam larval behavior in this study also causes differences in the temporal variances of larval along-shore drifting distances, with vertical sinking behavior decreasing the variance and swimming behavior increasing the variance (Fig. 9c). This is associated with the different turbulence scales near the surface and bottom of the water column, as larval sinking exposes larvae to deeper water with less turbulence and larval swimming exposes larvae close to surface water with stronger turbulence (Zhang et al., 2015).

In terms of the 'larval drift paradox', species with larvae that move unidirectionally downstream will tend to go extinct from the upstream edge of their distribution (Gaines et al., 2003; Shanks and Eckert, 2005; Byers and Pringle, 2006). If the model sensitivity prediction observed here is reflective of empirical trends, then for surfclams, increased downstream larval drift distances would further exacerbate this effect. Shanks and Eckert (2005) suggest the paradox can be solved by spreading spawning over times during which predominant currents move in different directions (e.g., seasonally shifting north versus south currents). The influence of seasonal variability of spawning on larval connectivity in surfclams is not addressed in this paper, but is the focus of a companion contribution (Zhang et al., 2015). In the case of surfclams, and other sympatric species with comparable larval duration (e.g., ocean quahogs and sea scallops), the paradox may be avoided because a gyre is present at the upstream end of the distribution in the Georges Bank region that facilitates self-recruitment to that 'upstream' extent of the population and thus maintains that upstream distribution, thereby preventing localized extinction at that upstream end of the population.

### 6.3. Coupled modeling system

In this study, a physical circulation model based on the Regional Ocean Modeling System (ROMS) was coupled with the surfclam larval individual based model to simulate surfclam larval transport. A few other larval transport modeling studies for benthic species along the U.S. northeast coast are also summarized and compared in Table 3, including those for the sea scallop (Tian et al., 2009), lobster (Incze and Naimie, 2000; Xue et al., 2008), and oyster (North et al., 2008; Haase et al., 2012; Narváez et al., 2012a, b). Comparison and evaluation of different physical circulation models is beyond the scope of this study (see for example, Leis et al., 2011). However, the differences in coupling methods, in particular "in-line" or "off-line", and inclusion of different larval behaviors merit further discussion here.

In this study, the physical circulation model was coupled with the surfclam larval model using an "in-line" method, which enables both models to be run simultaneously. Another typically used coupling method is "off-line", wherein both models are run separately. Both "in-line" and "off-line" coupling methods have their strengths and limitations, and no systematic comparison study has as yet been conducted. For "in-line" coupling, the biological model and the physical circulation model are run together for every time step (4 min in this study). Smaller spatial-scale and shorter time-scale physical processes such as tidal effects, sub-grid turbulence, etc., can be better resolved, which might potentially affect larval transport greatly, depending on the specific conditions of the physical environment simulated. The compensating drawback of "in-line" coupling is its additional computational cost, especially when a large number of larvae are released in the model. In "off-line" coupling, the hydrodynamic model output is stored and later interpolated and provided to a separate larval tracking model. This method is more computationally efficient and more convenient for sensitivity tests of larval behavior, release locations, diffusivity, etc., without the need to redo the hydrodynamic model calculation each time. However, the archived physical model output is often not stored in small enough time intervals so that the information provided to the larval tracking model might fail to resolve important small spatial-scale or short time-scale physical processes. The MAB and GBK are relatively more dynamic regions, especially the Southern New England shelf and the GBK where tidal effects are strong (Csanady and Magnell, 1987; He and Wilkin, 2006). Thus the "in-line" coupling method applied in this modeling system is likely to better resolve larval trajectories in these dynamic regions.

Besides larval growth required for surfclam larval settlement, both swimming and sinking behaviors were included in the larval model. Vertical behavior is found to be significant in determining surfclam larval drifting distances (Fig. 9) and mean connectivity patterns (not shown here), further confirming the importance of including behavior in the larval model. Generally larval growth and vertical swimming are the primary components of most larval models, although the relative importance of each differs in determining larval drifting distance, larval settlement success, larval transport patterns, etc. (Xue et al., 2008; Kim et al., 2010; Narváez et al., 2012a, b). Larval growth is itself intimately meshed with the larval vertical sinking rate and swimming speed, as each of these is a function of larval size and larval size is used as the criterion for larval settlement. Larval vertical swimming and sinking behaviors generally combine with background vertical advection and turbulent mixing to determine the position of the larvae in the water column, thereby determining the exposure of larvae to different temperature fields and water current velocities, and ultimately resulting in differential drifting distances (North et al., 2008; Tian et al., 2009). A sensitivity study focused on larval swimming behavior for two oyster species (*Crassostrea virginica* and *C. ariakensis*) in Chesapeake Bay demonstrated significant impacts on larval transport by influencing dispersal distances, transport success, and connectivity among different subpopulations (North et al., 2008). However, in some systems, the background vertical advection and turbulent vertical mixing might be strong enough to de-emphasize larval behavior effects. Such is the case for eastern oysters (*C. virginica*) in Mobile Bay, Alabama, and in Delaware Bay, New Jersey/Delaware (Kim et al., 2010; Narváez et al., 2012b). Off the northeastern U.S shelf in this study, surfclam larval behaviors interact with different underlying physical mechanisms to make a significant impact on their transport and to regional connectivity. More details of larval transport variations and larval behavior effects are presented in Zhang et al. (2015).

Habitat selection at larval settlement is another important component in larval models, especially for those species with high sensitivity to different substrates for larval settlement. In a study on sea scallops (*Placopecten magellanicus*) on GBK, this behavior was applied in the larval model in the form of varying settlement probabilities for different bottom substrates (Tian et al., 2009). In an oyster (*Ostrea chilensis*) larval transport study in Tasman Bay, a threshold of habitat quality and larval searching behavior were implemented in the larval model, so that the "landed" larvae could still return to the water column if the bottom substrate was not suitable and did not meet the quality threshold (Broekhuizen et al., 2011). For the Atlantic surfclam in this study, suitable habitat ranges from the Gulf of Maine south to Cape Hatteras of North Carolina, covering almost half of the MAB shelf and GBK in depths of 8–66 m. There is no obvious variation of surfclam habitat inside these regions, thus no need existed in this study to include habitat selecting behavior.

### 6.4. Model limitations

The Gulf Stream is one important current system known to have a significant impact on the MAB/GBK shelf water and its circulation properties, particularly through the formation of meanders and

eddies (Chen et al., 2014; Churchill et al., 1993; Gawarkiewicz et al., 2001; Rasmussen et al., 2005). One warm-core ring (WCR) off the Gulf Stream penetrating onto the MAB/GBK shelf might affect the water properties substantially with a duration lasting as long as several months. Accurately simulating the variability of the Gulf Stream, including the development of its meanders and warm-core rings has proven to be difficult, without further aid from more advanced modeling techniques such as data assimilation (Chen et al., 2014), etc. In our modeling system, although the main characters of the mean shelf current system are adequately captured by the circulation model, the full range of temporal and spatial variability might not be, especially along the shelf break where Gulf Stream meanders have a large impact (Fig. 3c, d). We cannot estimate the degree to which inaccuracies in the position and behavior of the Gulf Stream may affect surfclam larval trajectories, although we believe this influence is likely to be minor to the long-term mean pattern of larval transport and connectivity, for example the 4-year means examined in this study. The current grid resolution at 6–12 km in the physical circulation model might not be enough to resolve fine-scale features such as river plumes off estuaries, and the shelf break front and tidal front which correspond to sharp bathymetric changes. Generally river plumes are not thick and deep enough (Garvine, 1995) to affect surfclam larval transport, which usually stay close to or below the thermocline (Zhang et al., 2015). For the shelf break front, this model's low resolution in resolving the accurate bathymetry off the shelf break might cause errors in reproducing the right position of shelf-break front. However, most surfclam larvae generally stay on the shelf shallower than 60 m isobath, thus the shelf-break front at around 100 m isobath plays a minor role in affecting surfclam larval transport. For the tidal front off GBK edges with sharp bathymetric changes, this circulation model was found not able to get its position accurate enough. This feature is important for surfclam larval transport as it is directly related to the mechanism connecting the GBK and MAB surfclam populations. In the future, a more refined physical circulation model with higher resolution might be needed to better examine the GBK circulation and connectivity with MAB.

Inside the surfclam larval model, the food concentration is set at an optimal constant value, because we have insufficient information from field observations to provide an accurate and reliable time- and space-varying estimate to the model (e.g., Munroe et al., 2013). Once we have enough data to be able to construct a food climatology dataset for the model, improvements in model performance can be expected, but sensitivity results (not shown here) with modified food quality values indicate that the main larval transport and connectivity pattern is unchanged. This is largely due to saturation of larval feeding rate at relatively low planktonic algal densities. Apart from the assumed mortality due to unsuccessful settlement before 35 days or due to settlement into inappropriate water depths, planktonic daily mortality was not included in the current model. Sensitivity analyses using modified planktonic mortality (not shown here) likewise demonstrated that the main transport and connectivity patterns remain unchanged, but the magnitude of dispersal drops with increasing planktonic mortality. The larval release number from each region at each time is subject to large increase if connectivity among smaller regions will be examined, in order to obtain robust enough connectivity statistics. Also, more observational data of surfclam larval concentration or an estimate of surfclam connectivity from genetic studies might be needed for better model validation and evaluation.

## Acknowledgment

This study has been supported by the National Science Foundation project, “CNH: Collaborative Research: Climate Change and Responses in a Coupled Marine System (Award: GEO-0909484).” The authors are grateful to Larry Jacobson, Daniel Hennen, and Toni Chute from the National Marine Fisheries Service Northeast Fisheries Science Center for providing the surfclam survey data, and to industry advisors David Wallace and Thomas Hoff for fishery advice. The authors also thank Dr. John Wilkin and Dr. Julia Levin from Rutgers Institute of Marine and Coastal Sciences for their help in setting up the physical circulation model. This study also utilized data collected by the Northeast Fisheries Science Center as part of an ongoing mission to monitor and assess the Northeast Continental Shelf ecosystem, for the physical model surface and bottom temperature comparisons. The authors also thank the Rutgers Institute of Marine and Coastal Sciences Ocean Modeling Group for access to the ROMS model source code and providing the computational resources required for this study. Finally the authors would also thank the two anonymous reviewers for their thorough reviews, comments and suggestions to significantly improve this paper.

## References

Arnold, W.S., Hitchcock, G.L., Frischer, M.E., Wanninkhof, R., Sheng, Y.P., 2005. Dispersal of an introduced larval cohort in a coastal lagoon. Limnol. Oceanogr. 50, 587–597.

Ayata, S.D., Ellien, C., Dumas, F., Dubois, S., Thiébaut, É., 2009. Modelling larval dispersal and settlement of the reef-building polychaete *Sabellaria alveolata*: role of hydroclimatic processes on the sustainability of biogenic reefs. Cont. Shelf Res. 29, 1605–1623.

Backus, R.H., 1987. Geology. In: Backus, R.H. (Ed.), Georges Bank. MIT Press, Cambridge, MA, pp. 22–24.

Beardsley, R.C., Boicourt, W.C., 1981. On estuarine and continental shelf circulation in the Middle Atlantic Bight. In: Warren, B.A., Wunsch, C. (Eds.), Evolution of Physical Oceanography: Scientific Surveys in Honor of Henry Stommel. MIT Press, Cambridge, Mass, pp. 198–235.

Bleck, R., Halliwell Jr., G.R., Wallcraft, A.J., Carroll, S., Kelly, K., Rushing, K., 2002. Hybrid Coordinate Ocean Model (HYCOM) User's Manual: Details of the Numerical Code. Available from. http://hycom.rsmas.miami.edu.

Broekhuizen, N., Lundquist, C.J., Hadfield, M.G., Brown, S.N., 2011. Dispersal of oyster (*Ostrea chilensis*) larvae in Tasman Bay inferred using a verified particle tracking model that incorporates larval behavior. J. Shellfish Res. 30, 643–658.

Budgell, W.P., 2005. Numerical simulation of ice-ocean variability in the Barents Sea region. Ocean. Dyn. 55, 370–387.

Byers, J.E., Pringle, J.M., 2006. Going against the flow: retention, range limits and invasions in advective environments. Mar. Ecol. Prog. Ser. 313, 27–41.

Cargnelli, L.M., Griesbach, S.J., Packer, D.B., Weissberger, E., 1999. Atlantic surfclam, *Spisula solidissima*, Life History and Habitat Characteristics. National Oceanic and Atmospheric Administration Technical Memorandum NMFS-NE-142, p. 13.

Castelao, R., Glenn, S., Schofield, O., Chant, R., Wilkin, J., Kohut, J., 2008. Seasonal evolution of hydrographic fields in the central Middle Atlantic Bight from glider observations. Geophys. Res. Lett. 35, L03617. http://dx.doi.org/10.1029/2007GL032335.

Chen, C., Beardsley, R., Franks, P.J., 2001. A 3-D prognostic numerical model study of the Georges Bank ecosystem. Part I: physical model. Deep Sea Res. Part II: Top. Stud. Oceanogr. 48, 419–456.

Chen, K., He, R., 2010. Numerical investigation of the Middle Atlantic Bight shelf break frontal circulation using a high-resolution ocean hindcast model. J. Phys. Oceanogr. 40, 949–964.

Chen, K., He, R., Powell, B.S., Gawarkiewicz, G.G., Moore, A.M., Arango, H.G., 2014. Data assimilative modeling investigation of Gulf Stream Warm Core Ring interaction with continental shelf and slope circulation. J. Geophys. Res.-Oceans 119, 5968–5991. http://dx.doi.org/10.1002/2014JC009898.

Churchill, J.H., Levine, E.R., Connors, D.N., Cornillon, P.C., 1993. Mixing of shelf, slope and Gulf Stream water over the continental slope of the Middle Atlantic Bight. Deep Sea Res. Part I: Oceanogr. Res. Pap. 40, 1063–1085.

Cowen, R.K., Sponaugle, S., 2009. Larval dispersal and marine population connectivity. Annu. Rev. Mar. Sci. 1, 443–466.

Csanady, G.T., Magnell, B.A., 1987. Mixing processes. In: Backus, R.H. (Ed.), Georges Bank. MIT Press, Cambridge, MA, pp. 163–169.

Dekshenieks, M.M., Hofmann, E.E., Powell, E.N., 1993. Environmental effects on the growth and development of eastern oyster, *Crassostrea virginica* Gmelin, 1791, larvae: a modeling study. J. Shellfish Res. 12, 241–254.

Dekshenieks, M.M., Hofmann, E.E., Klinck, J.M., Powell, E.N., 1996. Modeling the vertical distribution of oyster larvae in response to environmental conditions. Mar. Ecol. Prog. Ser. 136, 97–110.

Fay, C.W., Neves, R.J., Pardue, G.B., 1983. Species Profiles. Life Histories and Environmental Requirements of Coastal Fishes and Invertebrates (Mid-Atlantic). Surfclam. Virginia Polytechnic Inst. and State Univ.. Dept. of Fisheries and Wildlife Sciences, Blacksburg (USA).

Fleming, N.E., Wilkin, J.L., 2010. MOCHA: A 3-D climatology of the temperature and salinity of the Middle Atlantic Bight. EOS Trans. AGU 91. Ocean Sci. Meet. Suppl., Abstract PO35G-08.
Gaines, S.D., Gaylord, B., Largier, J., 2003. Avoiding current oversights in marine reserve design. Ecol. Appl. 13, S32–S64.
Garvine, R.W., 1995. A dynamical system for classifying buoyant discharges. J. Cont. Shelf Res. 15, 1585–1596.
Gawarkiewicz, G., Bahr, F., Beardsley, R.C., Brink, K.H., 2001. Interaction of a slope eddy with the shelf break front in the Middle Atlantic Bight. J. Phys. Oceanogr. 31, 2783–2796.
Goldberg, R., 1989. Biology and Culture of the Surfclam. Chapter 10. In: Manzi, J.J., Castagna, M. (Eds.), Clam Mariculture in North America. Elsevier Science Publishers, Amsterdam, pp. 263–276.
Haase, A.T., Eggleston, D.B., Luettich, R.A., Weaver, R.J., Puckett, B.J., 2012. Estuarine circulation and predicted oyster larval dispersal among a network of reserves. Estuar. Coast. Shelf Sci. 101, 33–43.
Haidvogel, D.B., Arango, H.G., Hedstrom, K., Beckmann, A., Malanotte-Rizzoli, P., Shchepetkin, A.F., 2000. Model evaluation experiments in the North Atlantic Basin: simulations in nonlinear terrain-following coordinates. Dyn. Atmos. Oceans 32, 239–281.
Hare, M.P., Weinberg, J.R., 2005. Phylogeography of surfclams, *Spisula solidissima*, in the western North Atlantic based on mitochondrial and nuclear DNA sequences. Mar. Biol. 146, 707–716.
Hare, M.P., Weinberg, J., Peterfalvy, O., Davidson, M., 2010. The "southern" surfclam (*Spisula solidissima similis*) found north of its reported range: a commercially harvested population in Long Island Sound, New York. J. Shellfish Res. 29, 799–807.
He, R., Wilkin, J.L., 2006. Barotropic tides on the southeast New England shelf: a view from a hybrid data assimilative modeling approach. J. Geophys. Research-Oceans 111, C08002. http://dx.doi.org/10.1029/2005JC003254.
Hurley, D.H., Walker, R.L., 1996. The effects of larval stocking density on growth, survival, and development of laboratory-reared *Spisula solidissima similis* (Say, 1822). J. Shellfish Res. 15, 715–718.
Hurley, D.H., Walker, R.L., 1997. Effects of temperature and salinity upon larval growth, survival and development in hatchery reared southern Atlantic surfclams *Spisula solidissima similis*. J. World Aquac. Soc. 28, 407–411.
Hurley, D.H., Walker, R.L., O'Beirn, F.X., 1997. Growth and survival of *Spisula solidissima similis* larvae fed different rations of Tahitian strain *Isochrysis* species. J. Shellfish Res. 16, 151–156.
Incze, L.S., Naimie, C.E., 2000. Modelling the transport of lobster (*Homarus americanus*) larvae and postlarvae in the Gulf of Maine. Fish. Oceanogr. 9, 99–113.
Incze, L., Xue, H., Wolff, N., Xu, D., Wilson, C., Steneck, R., Chen, Y., 2010. Connectivity of lobster (*Homarus americanus*) populations in the coastal Gulf of Maine: part II. Coupled biophysical dynamics. Fish. Oceanogr. 19, 1–20.
Jones, D.S., 1981. Reproductive cycles of the Atlantic surf clam *Spisula solidissima*, and the ocean quahog *Arctica islandica* off New Jersey. J. Shellfish Res. 1, 23–32.
Johnson, K.B., Shanks, A.L., 2003. Low rates of predation on planktonic marine invertebrate larvae. Mar. Ecol. Prog. Ser. 248, 125–139.
Kim, C.K., Park, K., Powers, S.P., Graham, W.M., Bayha, K.M., 2010. Oyster larval transport in coastal Alabama: dominance of physical transport over biological behavior in a shallow estuary. J. Geophys. Research-Oceans 115, C10019. http://dx.doi.org/10.1029/2010JC006115.
Kim, Y., Powell, E.N., 2004. Surfclam histopathology survey along the Delmarva mortality line. J. Shellfish Res. 23, 429–442.
Largier, J.L., 2003. Considerations in estimating larval dispersal distances from oceanographic data. Ecol. Appl. 13, 71–89.
Leis, J.M., Van Herwerden, L., Patterson, H., 2011. Estimating connectivity in marine fish populations: what works best? Oceanogr. Mar. Biol. Annu. Rev. 49, 193–234.
Lentz, S.J., 2008. Observations and a model of the mean circulation over the Middle Atlantic Bight continental shelf. J. Phys. Oceanogr. 38, 1203–1221.
Levin, L.A., 2006. Recent progress in understanding larval dispersal: new directions and digressions. Integr. Comp. Biol. 46, 282–297.
López-Duarte, P., Carson, H.S., Cook, G.S., Fodrie, F.J., Becker, B.J., DiBacco, C., Levin, L.A., 2012. What controls connectivity? An empirical, multi-species approach. Integr. Comp. Biol. 52, 511–524.
Lough, R.G., Buckley, L.J., Werner, F.E., Quinlan, J.A., Pehrson Edwards, K., 2005. A general biophysical model of larval cod (*Gadus morhua*) growth applied to populations on Georges Bank. Fish. Oceanogr. 14, 241–262.
Lynch, D.R., Ip, J.T., Naimie, C.E., Werner, F.E., 1996. Comprehensive coastal circulation model with application to the Gulf of Maine. Cont. Shelf Res. 16, 875–906.
Lynch, D.R., Holboke, M.J., Naimie, C.E., 1997. The Maine coastal current: spring climatological circulation. Cont. Shelf Res. 17, 605–634.
Ma, H., Grassle, J.P., Chant, R.J., 2006a. Vertical distribution of bivalve larvae along a cross-shelf transect during summer upwelling and downwelling. Mar. Biol. 149, 1123–1138.
Ma, H., Grassle, J.P., Rosario, J.M., 2006b. Initial recruitment and growth of surfclams (*Spisula solidissima* Dillwyn) on the inner continental shelf of New Jersey. J. Shellfish Res. 25, 481–489.
Mann, R., Campos, B.M., Luckenbach, M.W., 1991. Swimming rate and responses of larvae of three mactrid bivalves to salinity discontinuities. Mar. Ecol. Prog. Ser. 68, 257–269.
Mellor, G.L., 2003. Users Guide for a Three-dimensional, Primitive Equation, Numerical Ocean Model. Princeton University, p. 53.
Mid-Atlantic Fishery Management Council, 2005. Overview of the Surfclam and Ocean Quahog Fisheries and Quota Considerations for 2006 and 2007. Mid-Atlantic Fishery Management Council, Dover, DE.
Miller, J.L., Lee, T.N., 1995. Gulf stream meanders in the south Atlantic bight: 1. Scaling and energetics. J. Geophys. Research-Oceans 100, 6687–6704.
Miller, T.J., 2007. Contribution of individual-based coupled physical-biological models to understanding recruitment in marine fish populations. Mar. Ecol. Prog. Ser. 347, 127–138.
Miller, S.H., Morgan, S.G., 2013. Interspecific differences in depth preference: regulation of larval transport in an upwelling system. Mar. Ecol. Prog. Ser. 476, 301–306.
Munroe, D.M., Powell, E.N., Mann, R., Klinck, J.M., Hofmann, E.E., 2013. Underestimation of primary productivity on continental shelves: evidence from maximum size of extant surfclam (*Spisula solidissima*) populations. Fish. Oceanogr. 22, 220–233.
Narváez, D.A., Klinck, J.M., Powell, E.N., Hofmann, E.E., Wilkin, J., Haidvogel, D.B., 2012a. Modeling the dispersal of eastern oyster (*Crassostrea virginica*) larvae in Delaware Bay. J. Mar. Res. 70, 381–409.
Narváez, D.A., Klinck, J.M., Powell, E.N., Hofmann, E.E., Wilkin, J., Haidvogel, D.B., 2012b. Circulation and behavior controls on dispersal of eastern oyster (*Crassostrea virginica*) larvae in Delaware Bay. J. Mar. Res. 70, 2–3.
North, E.W., Schlag, Z., Hood, R.R., Li, M., Zhong, L., Gross, T., Kennedy, V.S., 2008. Vertical swimming behavior influences the dispersal of simulated oyster larvae in a coupled particle-tracking and hydrodynamic model of Chesapeake Bay. Mar. Ecol. Prog. Ser. 359, 99–115. http://dx.doi.org/10.3354/meps07317.
Northeast Fisheries Science Center (NEFSC), 2010. 49th Northeast Regional Stock Assessment Workshop (49th SAW) Assessment Report. United States Department of Commerce. Northeast Fisheries Science Center Reference Document. 10-03; 383p.
O'Connor, M.I., Bruno, J.F., Gaines, S.D., Halpern, B.S., Lester, S.E., Kinlan, B.P., Weiss, J.M., 2007. Temperature control of larval dispersal and the implications for marine ecology, evolution, and conservation. Proc. Natl. Acad. Sci. 104, 1266–1271.
O'Reilly, J.E., Evans-Zetlin, C., Busch, D.A., 1987. Primary production. In: Backus, R.H. (Ed.), Georges Bank. MIT Press, Cambridge, MA, pp. 220–223.
Peck, M.A., Hufnagl, M., 2012. Can IBMs tell us why most larvae die in the sea? Model sensitivities and scenarios reveal research needs. J. Mar. Syst. 93, 77–93.
Powell, T.M., Lewis, C.V., Curchitser, E.N., Haidvogel, D.B., Hermann, A.J., Dobbins, E.L., 2006. Results from a three-dimensional, nested biological-physical model of the California Current System and comparisons with statistics from satellite imagery. J. Geophys. Research-Oceans 111, C07018. http://dx.doi.org/10.1029/2004JC002506.
Quijón, P.A., Grassle, J.P., Rosario, J.M., 2007. Naticid snail predation on early post-settlement surfclams (*Spisula solidissima*) on the inner continental shelf of New Jersey, USA. Mar. Biol. 150, 873–882.
Rasmussen, L.L., Gawarkiewicz, G., Owens, W.B., Lozier, M.S., 2005. Slope water, Gulf Stream, and seasonal influences on southern Mid-Atlantic Bight circulation during the fall-winter transition. J. Geophys. Research-Oceans 110, C02009. http://dx.doi.org/10.1029/2004JC002311.
Renaud, S.M., Thinh, L.V., Lambrinidis, G., Parry, D.L., 2002. Effect of temperature on growth, chemical composition and fatty acid composition of tropical Australian microalgae grown in batch cultures. Aquaculture 211, 195–214.
Reynolds, R.W., Smith, T.M., Liu, C., Chelton, D.B., Casey, K.S., Schlax, M.G., 2007. Daily high-resolution-blended analyses for sea surface temperature. J. Clim. 20, 5473–5496.
Reyns, N.B., Eggleston, D.B., Luettich, R.A., 2006. Secondary dispersal of early juvenile blue crabs within a wind-driven estuary. Limnol. Oceanogr. 51, 1982–1995.
Reyns, N.B., Eggleston, D.B., Luettich, R.A., 2007. Dispersal dynamics of post-larval blue crabs, *Callinectes sapidus*, within a wind-driven estuary. Fish. Oceanogr. 16, 257–272.
Roosenburg, W.H., Wright, D.A., Castagna, M., 1984. Thermal tolerance by embryos and larvae of the surf clam, *Spisula solidissima*. Environ. Res. 34, 162–169.
Ropes, J.W., 1968. Reproductive cycle of the surf clam, *Spisula solidissima*, in offshore New Jersey. Biol. Bull. 135, 349–365.
Ropes, J.W., 1980. Biological and Fisheries Data on the Atlantic Surf Clam, *Spisula solidissima*. Department of Commerce, National Marine Fisheries Service, United States, p. 99. Northeast Fisheries Science Center Technical Series Report No. 24.
Rumrill, S.S., 1990. Natural mortality of marine invertebrate larvae. Ophelia 32, 163–198.
Savina, M., Ménesguen, A., 2008. A deterministic population dynamics model to study the distribution of a benthic bivalve with planktonic larvae (*Paphia rhomboides*) in the English Channel (NW Europe). J. Mar. Syst. 70, 63–76.
Schofield, O., Chant, R., Cahill, B., Castelao, R., Gong, D., Kahl, A., Kohut, J., Montes-Hugo, M., Ramadurai, R., Ramey, P., Yi, X., Glenn, S.M., 2008. Seasonal forcing of primary productivity on broad continental shelves. Oceanography 21, 104–117.
Shanks, A.L., 2009. Pelagic larval duration and dispersal distance revisited. Biol. Bull. 216, 373–385.
Shanks, A.L., Brink, L., 2005. Upwelling, downwelling, and cross-shelf transport of bivalve larvae: test of a hypothesis. Mar. Ecol. Prog. Ser. 302, 1–12.
Shanks, A.L., Eckert, G., 2005. Life–history traits and population persistence of California Current fishes and benthic crustaceans: solution of a marine drift paradox. Ecol. Monogr. 75, 505–524.

Shchepetkin, A.F., McWilliams, J.C., 1998. Quasi-monotone advection schemes based on explicit locally adaptive dissipation. Mon. Weather Rev. 126, 1541–1580.
Shchepetkin, A.F., McWilliams, J.C., 2003. A method for computing horizontal pressure-gradient force in an oceanic model with a nonaligned vertical coordinate. J. Geophys. Research-Oceans 108 (C3), 3090. http://dx.doi.org/10.1029/2001JC001047.
Shchepetkin, A.F., McWilliams, J.C., 2005. The regional oceanic modeling system (ROMS): a split-explicit, free-surface, topography-following-coordinate oceanic model. Ocean. Model. 9, 347–404.
Short, J., Metaxas, A., Daigle, R.M., 2013. Predation of larval benthic invertebrates in St. George's Bay, Nova Scotia. J. Mar. Biol. Assoc. U. K. 93, 591–599.
Tian, R., Chen, C., Stokesbury, K.D.E., Rothschild, B.J., Xu, Q., Hu, S., Marino II, M.C., 2009. Modeling exploration of the connectivity between sea scallop populations in the Middle Atlantic Bight and over Georges Bank. Mar. Ecol. Prog. Ser. 380, 147–160.
Tilburg, C.E., Seay, J., Bishop, T.D., Miller III, H.L., Meile, C., 2010. Distribution and retention of Petrolisthes armatus in a coastal plain estuary: the role of vertical movement in larval transport, Estuarine. Coast. Shelf Sci. 88, 260–266.
Underwood, A.J., Keough, M.J., 2001. Supply-side ecology: the nature and consequences of variations in recruitment of intertidal organisms. In: Bertness, M.D., Gaines, S.D., Hay, M.E. (Eds.), Marine Community Ecology. Sinauer Associates, Sunderland, pp. 183–200.
Walker, R.L., Hurley, D.H., Kupfer, R., 1998. Growth and survival of Atlantic surfclam, *Spisula solidissima*, larvae and juveniles fed various microalga diets. J. Shellfish Res. 17, 211–214.
Walker, R.L., O'Beirn, F.X., 1996. Embryonic and larval development of *Spisula solidissima similis* (Say, 1822) (Bivalvia: Mactridae). Veliger 39, 60–64.
Wang, Z., Haidvogel, D.B., Bushek, D., Ford, S.E., Hofmann, E.E., Powell, E.N., Wilkin, J., 2012. Circulation and water properties and their relationship to the oyster disease MSX in Delaware Bay. J. Mar. Res. 70, 2–3.
Warner, J.C., Geyer, W.R., Lerczak, J.A., 2005. Numerical modeling of an estuary: a comprehensive skill assessment. J. Geophys. Research-Oceans 110, C05001. http://dx.doi.org/10.1029/2004JC002691.
Weinberg, J.R., Dahlgren, T.G., Halanych, K.M., 2002. Influence of rising sea temperature on commercial bivalve species of the U.S. Atlantic coast. Am. Fish. Soc. Symposium 32, 131–140.
Weinberg, J.R., 2005. Bathymetric shift in the distribution of Atlantic surfclams: response to warmer ocean temperatures. ICES J. Mar. Sci. 62, 1444–1453.
Weinberg, J.R., Powell, E.N., Pickett, C., Nordahl Jr., V.A., Jacobson, L.D., 2005. Results from the 2004 Cooperative Survey of Atlantic Surfclams. Northeast Fishery Science Center Reference Documents 05-01, pp. 1–41.
Werner, F.E., Page, F.H., Lynch, D.R., Loder, J.W., Lough, R.G., Perry, R., Greenberg, David A., Sinclair, M.M., 1993. Influences of mean advection and simple behavior on the distribution of cod and haddock early life stages on Georges Bank. Fish. Oceanogr. 2, 43–64.
Wright, D.A., Kennedy, V.S., Roosenburg, W.H., Castagna, M., Mihursky, J.A., 1983. Temperature tolerance of embryos and larvae of five bivalve species under simulated power plant entrainment conditions: a synthesis. Mar. Biol. 77, 271–278.
Xue, H., Incze, L., Xu, D., Wolff, N., Pettigrew, N., 2008. Connectivity of lobster populations in the coastal Gulf of Maine: Part I: circulation and larval transport potential. Ecol. Model. 210, 193–211.
Zhang, X., Haidvogel, D.B., Munroe, D., Powell, E.N., 2015. Modeling larval connectivity of the Atlantic surfclams within the Middle Atlantic Bight: Model development, larval dispersal and metapopulation connectivity. Estuarine, Coastal and Shelf Science 153, 38–53.